

Hakan Sarioglu‡§, Stefanie Brandner‡, Markus Haberger‡, Carola Jacobsen‡, Josef Lichtmannegger‡, Mark Wormke‡, and Ulrich Andrae‡¶

As part of a comprehensive survey of the impact of the environmental pollutant and hepatocarcinogen 2,3,7,8tetrachlorodibenzo-p-dioxin (TCDD) on the proteome of hepatic cells, we have performed a high resolution twodimensional gel electrophoresis study on the rat hepatoma cell line 5L. 78 protein species corresponding to 73 different proteins were identified as up- or down-regulated following exposure of the cells to 1 nm TCDD for 8 h. There was an overlap of only nine proteins with those detected as altered by TCDD in our recent study using the non-gel-based isotope-coded protein label method (Sarioglu, H., Brandner, S., Jacobsen, C., Meindl, T., Schmidt, A., Kellermann, J., Lottspeich, F., and Andrae, U. (2006) Quantitative analysis of 2,3,7,8-tetrachlorodibenzo-p-dioxin-induced proteome alterations in 5L rat hepatoma cells using isotope-coded protein labels. Proteomics 6, 2407-2421) indicating a strong complementarity of the two approaches. For the majority of the altered proteins, an effect of TCDD on their abundance or posttranslational modifications had not been known before. Several observations suggest that a sizable fraction of the proteins with altered abundance was induced as an adaptive response to TCDD-induced oxidative stress that was demonstrated using the fluorescent probe dihydrorhodamine 123. A prominent group of these proteins comprised various enzymes for which there is evidence that their expression is regulated via the Keap1/Nrf2/antioxidant response element pathway. Other proteins included several involved in the maintenance of mitochondrial energy production and the regulation of the mitochondrial apoptotic pathway. A particularly intriguing finding was the up-regulation of the mitochondrial outer membrane pore protein, voltage-dependent anion channel-selective protein 2 (VDAC2), which was dependent on the presence of a functional aryl hydrocarbon receptor. The regulatability of VDAC2 protein abundance has not been described previously. In view of the recently discovered central role of VDAC2 as an inhibitor of the activation of the proapoptotic protein BAK and the mitochondrial apoptotic pathway, the present data point to a hitherto unrecognized mechanism by which TCDD may affect cellular homeostasis and survival. *Molecular & Cellular Proteomics* 7:394–410, 2008.

environmental contaminant 2,3,7,8-tetrachlorodibenzo-p-dioxin (TCDD)¹ is the prototype of a class of compounds known as halogenated aromatic hydrocarbons that includes dibenzo-p-dioxins, dibenzofurans, and polychlorinated biphenyls. TCDD has been shown to cause a wide variety of toxic effects and is regarded as the most potent hepatocarcinogen in experimental animals (1). Epidemiological evidence suggests that TCDD is also a human carcinogen (2, 3). The molecular mechanisms underlying the tumorigenic activity of the compound are still largely unknown, which strongly hampers the estimation of the risk to humans associated with dioxin exposure and necessitates further studies aimed at the clarification of these mechanisms. Moreover the multifaceted toxicity of TCDD makes it a very attractive model compound for studies addressing the identification of basic principles associated with the disturbance of cellular homeostasis.

From the Institutes of ‡Toxicology and §Human Genetics, GSF-Research Center for Environment and Health, D-85764 Neuherberg, Germany

Received, June 1, 2007, and in revised form, August 23, 2007 Published, MCP Papers in Press, November 12, 2007, DOI 10.1074/mcp.M700258-MCP200

¹ The abbreviations used are: TCDD, 2,3,7,8-tetrachlorodibenzo-*p*-dioxin; AFAR1, aflatoxin B1-aldehyde reductase; AhR, aryl hydrocarbon receptor; AHRE, aryl hydrocarbon response element; ALDH3A1, aldehyde dehydrogenase 3A1; ANT1, ADP/ATP translocase 1; ARE, antioxidant response element; ARNT, AhR nuclear translocator; CCT, chaperonin containing t-complex polypeptide 1; CYP, cytochrome P450; 2-DE, two-dimensional gel electrophoresis; DHR123, dihydrorhodamine 123; DTE, dithioerythritol; EROD, 7-ethoxyresorufin *O*-deethylase; HK, hexokinase; ICPL, isotope-coded protein label; JNK, c-Jun N-terminal kinase; NQO1, NAD(P)H:quinone oxidoreductase 1; Nrf2, nuclear factor E2 p45-related factor 2; PTM, posttranslational modification; R123, rhodamine 123; ROS, reactive oxygen species; TCP1, t-complex polypeptide 1; VDAC, voltage-dependent anion channel-selective protein.

TCDD is a ligand of the aryl hydrocarbon receptor (AhR), and it is assumed that most, if not all, toxic effects of TCDD are mediated by the AhR (4). Binding of TCDD to the cytosolic receptor results in the translocation of the ligand receptor complex into the cell nucleus and the dimerization with a related protein, the AhR nuclear translocator (ARNT). This heterodimer can act as a ligand-activated transcription factor by binding to a specific DNA sequence known as aryl hydrocarbon response element I (AHRE-I), xenobiotic-responsive element, or dioxin-responsive element, an enhancer located in regulatory regions of aryl hydrocarbon-responsive genes. Binding to the AHRE-I activates the transcription of target genes and thus results in an alteration of gene expression (5). In addition, the liganded AhR/ARNT heterodimer can function as a ligand-activated coactivator of the transcription of a different set of responsive genes via the interaction with another response element called AHRE-II (6, 7). TCDD-induced changes in gene expression may also occur indirectly as a consequence of an AhR/ARNT-dependent induction of oxidative stress and the transcriptional activation of still another set of genes via a different enhancer, the so-called antioxidant response element (ARE) (8). Moreover several AhR-dependent mechanisms not involving heterodimer binding to an AHRE have been suggested to contribute to the toxicity of TCDD (9-11). Thus, the mechanisms by which TCDD may interfere with signaling pathways appear to be extremely complex, and the elucidation of the resulting alterations in gene expression and their importance for the various aspects of TCDD toxicity clearly remains a continuing challenge.

The alterations in gene expression at the level of the transcriptome in hepatic cells exposed to TCDD have been explored in a number of studies on hepatoma cell lines from different species (12–14) and on rodents (7, 15–20). These studies have provided a large body of information on the effects of TCDD on gene expression at the mRNA level. There are, however, well documented, strong limitations regarding the correlation between mRNA and protein levels, and for the vast majority of the observed changes in mRNA abundance it has remained open to question whether they are of biological relevance because it is not known whether they are actually translated into changes of the abundance of their cognate proteins, *i.e.* at the functional level.

Studies on the effects of TCDD on hepatic cells of mammals at the level of the proteome are still scarce. Three *in vivo* investigations have dealt with the effects of dioxin on the protein profile of rats (21, 22) and marmosets (23). Although a comparison of the obtained results is difficult or even impossible because of the use of, in part, different species, rat strains, application routes, doses, and exposure periods, it is evident that relatively low numbers (up to a maximum of 10) of up- or down-regulated proteins were detected in the individual studies. This might reflect a limited biological activity of TCDD *in vivo* under the experimental conditions used, but it appears more likely that the low numbers were due to tech-

nical limitations of the *in vivo* approach. A major limiting factor of the studies, which all used two-dimensional gel electrophoresis (2-DE) for protein separation, may have been the use of IPG strips covering the broad pH range from 3 to 10 in all of these investigations. Unfortunately the use of these low resolution strips is almost mandatory for *in vivo* studies because the necessity to use reasonably large groups of animals to account for the unavoidable variability between individual animals practically precludes the use of combinations of the much better resolving IPG strips covering overlapping, narrow pH ranges (24, 25).

With the objective to obtain detailed insight into the proteome changes induced by TCDD in hepatic cells and to obtain new clues to the signaling pathways mediating its cellular activity, we are currently performing a series of in vitro studies aimed at characterizing the changes in protein abundance and posttranslational protein modifications in TCDDtreated 5L rat hepatoma cells. 5L cells are epithelial-like cells that express both the AhR and the ARNT protein. They are highly responsive to the toxic effects of TCDD, and they have been used in investigations on the role of AhR and ARNT in TCDD toxicity, cell cycle regulation, and cell signaling (11, 26-33) and on the induction of xenobiotic-metabolizing enzymes by TCDD (34). Moreover they have been successfully used in projects aiming at the identification of novel target genes of the AhR (14, 35). We recently reported results of a proteomics study in which the effects of TCDD on 5L cells were investigated using an LC-based mass spectrometric approach, the so-called isotope-coded protein label (ICPL) method (36, 37). In this study, we identified 89 protein species of various functional categories as up- or down-regulated by TCDD. It was likely, however, that the identified proteins represented only a fraction of the proteins actually altered by TCDD because several studies dealing with the detection of differentially expressed proteins by diverse techniques for quantitative proteome analysis reported a very limited overlap of the proteins identified by the different approaches (38, 39). It thus appeared expedient to complement our findings with results obtained by an experimental system for proteome analysis unrelated to the ICPL approach.

We have therefore conducted a quantitative proteomics analysis of the proteome alterations induced by TCDD in 5L cells using a gel-based approach, the classical 2-DE for protein separation and quantitation in combination with mass spectrometry for protein identification. To optimize protein resolution, separation of the proteins in the first dimension, *i.e.* by IEF, was performed on four individual gel strips with different narrow, overlapping IPGs covering a total pH range of 3–11. This approach has been shown to considerably increase the number of proteins detectable in comparison with the IPG strips of pH 3–10 or 4–7 most frequently used in 2-DE analyses and, thus, to yield a much more detailed picture of the proteome under study (24, 25).

EXPERIMENTAL PROCEDURES

Reagents

TCDD (purity >99%) in Me₂SO was obtained from Ökometric (Bayreuth, Germany). All chemicals and solvents used were of the highest purity available.

Cells

The 5L cell line is a variant of the Fao line (40), a descendant of the cell line H4lIEC3 established by Pitot *et al.* (41) from the Reuber H35 rat hepatoma (42). BP8 cells represent a variant clone of 5L cells that lacks the AhR (26, 29). Cells were grown as monolayers in 10-cm culture dishes containing RPMI 1640 medium supplemented with 10% FCS, 100 units/ml penicillin, and 100 μ g/ml streptomycin ("complete RPMI 1640 medium") at 37 °C in a humidified atmosphere of 95% air and 5% CO₂.

Treatment of the Cells with TCDD

Cells were seeded at a density of 1.5×10^6 cells/10-cm dish in complete RPMI 1640 medium. 24 h later, the medium was replaced by 5 ml of fresh complete RPMI 1640 medium, and 48 h after seeding 1 nm TCCD dissolved in Me₂SO or solvent alone was added for the times indicated. The Me₂SO concentration in the medium was 0.1%.

Harvest and Solubilization of Cells for 2-DE

After incubation, the medium was removed, and cells were washed three times with ice-cold PBS without Ca²⁺/Mg²⁺. To detach the cells from the plates, the monolayers were exposed to 3 ml of trypsin/EDTA at room temperature, the trypsin was removed completely, and the cells were detached by vigorous tapping of the plates on the table. The cells were rinsed off the plates with 3 ml of PBS-Ca²⁺/Mg²⁻ (three times) and pelleted by centrifugation (0 $^{\circ}$ C for 5 min at 1000 \times g). The cell pellet was carefully resuspended in 1 ml of $0.5 \times PBS$ without Ca2+/Mg2+ (0 °C) and centrifuged again (0 °C for 5 min at 1000 rpm). The cell pellet was then covered with 500 μ l of solubilization buffer at room temperature and immediately vortexed until the cells had dissolved completely. Solubilized cells from four identically treated dishes were each combined. The solubilization buffer contained 7 м urea, 2 м thiourea, 2% (w/v) CHAPS, 65 mм DTE for IPG strips pH 3.0-5.6 and 5.3-6.5 or 15 mm DTE for pH 6.2-7.5 and 7-11 (see below), 0.4% (w/v) Biolyte pH 3-10 (Bio-Rad), 0.4% (w/v) Pharmalyte pH 3-10 (Amersham Biosciences), and one protease inhibitor tablet (Complete, Roche Applied Science)/50 ml of buffer. Before use, a stock solution of urea and thiourea was treated with a mixed-bed ion exchanger (1% (w/v) Serdolit MB-1; Serva, Heidelberg, Germany) to remove ionic impurities.

Two-dimensional Gel Electrophoresis

2-DE was performed essentially as described by Görg et al. (25). In every experiment four samples for each pH range and treatment condition (TCDD or Me_2SO) were processed in parallel. Proteins were separated in the first dimension by IEF in a Multiphor II or IPGphor apparatus (Amersham Biosciences) using four different types of 24-cm IPG strips (Amersham Biosciences) covering pH ranges of 3.0–5.6, 5.3–6.5, 6.2–7.5, and 7–11. The strips were rehydrated in rehydration cassettes (Amersham Biosciences) with buffer containing 6 M urea and 2 M thiourea (pretreated with 1% (W/V) Serdolit MB-1), 1% (V/V) CHAPS, the appropriate IPG buffer (0.2%, W/V), a trace of bromphenol blue, and, depending on the pH range of the strips, 15 mM DTE for pH ranges 3.0–5.6 and 5.3–6.5 or 15 mg/ml DeStreak (Amersham Biosciences) for pH ranges pH 6.2–7.5 and 7–11. The IPG buffers used were 3.5–5.0 for pH range 3.0–5.6, 5.5–6.7 for pH range

5.3–6.6, 6–11 for pH range 6.2–7.5, and 7–11 for pH range 7–11. Following overnight rehydration of the strips, they were placed in the Multiphor II or IPGphor apparatus, and protein samples (100 μ l) were applied to the IPG strips by cup loading at the anodic end (IPG strips pH 5.3–6.5, 6.2–7.5, and 7–11) or the cathodic end (pH 3.0–5.6). 250 μ g of protein were applied with the exception of the pH 7–11 strips, which were run with 100 μ g of protein. IPG strips were subjected to IEF at 20 °C for 95 kV-h (pH 3–5.6), 150 kV-h (pH 5.3–6.5 and pH 6.2–7.5), and 100 kV-h (pH 7–11). The focusing protocols included a change of the electrode strips at low voltage to remove most of the salts in the samples.

For reduction and alkylation of the proteins, the IPG strips were equilibrated for 15 min in a solution of 50 mm Tris-HCl (pH 6.8), 6.0 m urea, 30% (v/v) glycerol, and 2% (w/v) SDS containing 1% (w/v) DTE and then for an additional 15 min in the same solution except that DTE was replaced by 4% (w/v) iodoacetamide. After equilibration, proteins were separated on SDS-polyacrylamide gels (12% T, 2.6% C) at 20 °C using the Ettan DALT II separation unit (Amersham Biosciences) (3 watts/gel for the first 30 min and 18 watts/gel until the end). The running buffer consisted of 50 mm Tris-HCl (pH 8.8), 386 mm glycine, and 2% (w/v) SDS. The Precision Plus Protein Standard (Bio-Rad) was used as molecular weight marker.

Protein Staining and 2-DE Gel Image Analysis

Gels were stained with the fluorescent dye ruthenium(II)-tris(bathophenanthrolinedisulfonate) as described by Lamanda *et al.* (43). Stained gels were scanned with the Fuji FLA-3000 phosphorimaging system (Raytest) using the software BASReader Version 3.01 with the following parameters: resolution, 100 μ m; 16-bit image (65,536 gray levels); sensitivity, 100; excitation wavelength, 473 nm; detection filter, O580.

For detection and quantitation of protein spots and comparison of gels, Proteomweaver software (release 4.0.0.5 beta, Bio-Rad) was used. The following parameters were used for spot detection: minimum spot radius limit of 4, minimum spot intensity (volume above base level) of 2000, and minimum contrast limit (height above base level) of 40. Gels from each experiment were processed by pairmatch-based normalization. Subsequently protein spots of every gel of both groups were automatically matched with each other, and the matching was carefully checked manually and corrected in case of obvious mismatches to avoid assigning false positives. To identify significant differences in spot intensities between the two groups the following rules were established: only spots matched in at least 50% of the gel images in a group were considered, and to get reasonable protein amounts for mass spectrometric identification only spots exceeding an average intensity threshold of 0.2 were taken for further analysis. The remaining spots were sorted according to their regulation factors, and for each experimental set the threshold regulation factor for the significance level (p < 0.05) was determined by the software using Student's t test. Differences were considered significant at p < 0.05 corresponding to a thresholding for 1.54-fold changes in spot intensities (i.e. 1.54 for up-regulation and 0.65 for down-regulation). Only spots exhibiting intensities significantly changed after TCDD treatment were further considered as candidate spots and subsequently subjected to manual verification.

Protein Identification by Mass Spectrometry

In-gel Proteolysis—Protein spots with altered intensities were selected for identification and, following silver staining of the 2-DE gels using a modification of the mass spectrometry-compatible version of Shevchenko et al. (44), manually excised with a scalpel. The gel pieces were washed with buffer containing 50 mm NH₄HCO₃ in 30% ACN, destained with 30 mm potassium hexacyanoferrate(III) and 100

mm sodium thiosulfate, and washed again with 50 mm $\rm NH_4HCO_3$ in 30% ACN. The pieces were shrunk with 100% (v/v) ACN prior to proteolytic digestion. Following addition of 0.2–0.4 mg of modified trypsin (Promega, Madison, WI), proteolysis was performed overnight at 37 °C. The supernatant was collected and combined with the eluates of two subsequent elution steps with 80% (v/v) ACN and 1% (v/v) TFA. The combined eluates were dried in a SpeedVac centrifuge and dissolved in 5–10 μ l of 70% (v/v) ACN and 0.1% (v/v) TFA. Samples that did not yield successful protein identifications in the subsequent MS analysis were reanalyzed after desalting and concentrating peptides with ZipTip® pipette tips containing C₁₈ reversed-phase medium (Millipore, Billerica, MA).

MS Analysis-Mass spectra were acquired using a Proteomics Analyzer 4700 (MALDI-TOF/TOF) mass spectrometer (Applied Biosystems, Framingham, MA). Measurements were performed with a 355 nm neodymium-doped yttrium aluminium garnet (Nd:YAG) laser in positive reflector mode with a 20-kV acceleration voltage. For each MS and MS/MS spectrum, 3000 shots in a m/z window of 800-4000 were accumulated. To obtain a mass accuracy better than 50 ppm, internal calibration using peptides resulting from autoproteolysis of trypsin (2163.05 and 2211.10 Da) was utilized. In addition, external calibration in the mass range from 800 to 3000 with a peptide mass standard consisting of eight peptides (Bruker, Billerica, MA) was used. For sample preparation, 0.5-µl aliquots of the digests were spotted on a target, dried, and mixed 1:1 with matrix consisting of 2 mg/ml α -cyano-4-hydroxycinnamic acid in 70% (v/v) ACN and 0.1% (v/v) TFA. Peak labeling was automatically done by 4000 series Explorer software Version 3.6 (Applied Biosystems) without any kind of smoothing of the peaks or base line. In addition to peptide mass fingerprint spectra, the five most abundant precursor ions having a signal-to-noise ratio higher than 70 were chosen for MS/MS fragmentation, which was performed using medium collision energy. An exclusion list of known contaminant ion masses of keratin and trypsin was used.

Data Processing-The processing of spectra obtained with the 4700 Proteomics Analyzer was carried out with the software GPS ExplorerTM Version 3.6 (Applied Biosystems). The combined MS and MS/MS spectra were searched against the Swiss-Prot (230,133 sequences, 84,471,903 residues; date July, 25, 2006) and the National Center for Biotechnology Information non-redundant (NCBInr) databases (4,878,246 sequences, 1,686,729,293 residues; date April 26, 2007) using an in-house version of the Mascot (Version 2.0) search engine (Matrix Science Ltd., London, UK) with the following parameters. One miscleavage was allowed. As taxon we chose Rattus, and as enzyme we chose trypsin. Carbamidomethylation of cysteine was set as fixed modification, and oxidation of methionine was set as variable modification. For MS spectra, mass errors of 65 ppm for precursor ions and 0.3 Da for fragment ions were allowed. For MS/MS of peptides, further filtering criteria were applied: the maximum peptide rank was set at 3, and the minimum ion score was set at 30% confidence level, which corresponds to a Mascot score of 10-12.

Criteria for Protein Identification—The GPS Explorer 3.6 software reports three different scores: The Mascot best ion score, *i.e.* the highest score of a single peptide; a total ion score, *i.e.* the sum of all peptide scores of one protein; and a protein score that includes a score for the peptide mass fingerprint in addition to the total ion score. The significance level is usually >20 for a peptide score and >40–50 for a protein score. Because different database searches have different Mascot significance levels due to different databases sizes and different numbers of masses submitted for a search, scores cannot be compared directly. For this reason, the software calculates a confidence interval from Mascot protein scores or ion scores, and the Mascot significance level for each search is defined as the 95% confidence level. Therefore, the total protein score confidence level is

a reliable and comparable parameter for the significance of a database search.

A protein was regarded as identified if the following three criteria were fulfilled. (i) The probability-based MOWSE (molecular weight search) protein score was above the 5% significance threshold for the respective database (95% confidence level). (ii) The matched peptide masses were abundant in the spectrum. (iii) The theoretical pl and the molecular mass of the protein suggested by the search result could be correlated with the position of the corresponding spot in the 2-DE gel. If the latter was not the case, posttranslational modifications (PTMs) were taken into consideration. In most cases only rank 1 proteins were identified for each 2-DE spot as the peptides of the proteins of the following rank positions were carefully searched for peptides shared with the identified protein. Additional protein hits were only included in the protein list when a significant score of the non-shared peptides was obtained. In the case where all peptides detected were shared by individual proteins, as was the case for e.g. myosin regulatory light chain 2-B and 2-A isoforms, this ambiguity was clearly marked in the tables.

A summary table is available as supplemental Table S1. MS/MS data for each peptide match including precursor masses with observed mass errors, peptide sequences, ion scores, ion score confidence levels, and modifications are listed. Only MS/MS data of peptides with an ion score confidence level higher than 95% are shown.

Western Blot Analysis

For Western blot analysis of VDAC2 abundance, cells were lysed in Cell Extraction Buffer (BIOSOURCE, Camarillo, CA), and 10 μg of total protein were resolved on 12% polyacrylamide gels (Protean II XL, Bio-Rad) and blotted onto PVDF membranes. VDAC2 was detected using polyclonal anti-VDAC2 antibodies (ab22170 or ab37985, Abcam, Cambridge, UK), a horseradish peroxidase-labeled secondary antibody, and ECL detection kit (Amersham Biosciences). The actin band, which served as loading control, was detected using an anti-actin antibody (clone AC-40, Sigma).

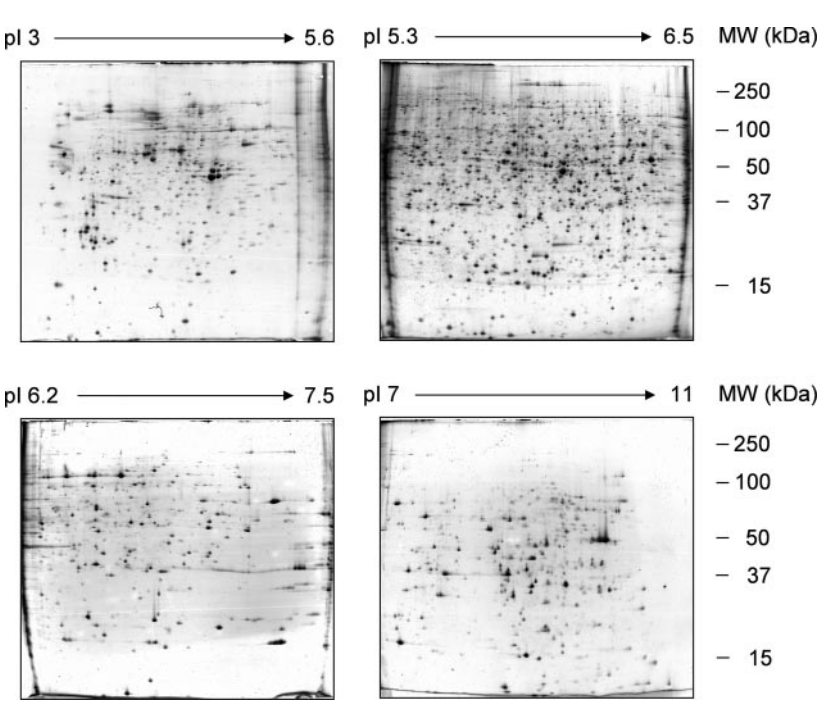
Real Time Quantitative PCR

The expression of VDAC2 and cytochrome P4501A1 (CYP1A1) at the mRNA level was quantitated by real time quantitative PCR with a LightCycler instrument (Roche Applied Science) using the following primers: VDAC2: forward, 5'-TTGGAGTGGGCTATACTCAGACT-3'; reverse, 5'-GCATTAAAGCTCTTCCCGTCT-3'; CYP1A1: forward, 5'-CCTTGGAGCTGGGTTTG-3'; reverse, 5'-GCTGTGGGGGATGGTGA-A-3'.

Measurement of the Generation of Reactive Oxygen Species

The formation of reactive oxygen species (ROS) in 5L cells was determined by measuring the intracellular oxidation of dihydrorhodamine 123 (DHR123) (Invitrogen-Molecular Probes) to the fluorescent rhodamine 123 (R123) by flow cytometry. Cells were exposed to 1 nm TCDD for 8 h as described above or to 50 μ M menadione for 30 min, and 15 min before the end of the exposure DHR123 was added to a final concentration of 5 μ M. Cells were rinsed with PBS, harvested with trypsin, and immediately placed on ice for flow cytometry, 5000 cells were analyzed on an LSR II flow cytometer (BD Biosciences) using excitation at 488 nm and a 530/30-nm band pass filter for detection. Autofluorescence was determined on 5L cells incubated without the dye and used for background subtraction. Populations of viable single cells (based on forward sideward scatter) were gated identically for ROS determinations for each treatment group. Mean fluorescence values were acquired using BD FACSDiva software and used for quantitative analysis. Histogram overlays were performed

Fig. 1. Representative fluorescently stained 2-DE gels of 5L cell lysates. Cells were treated with Me₂SO for 8 h and solubilized, and aliquots of the lysates were analyzed by 2-DE using four different 24-cm IPG strips covering overlapping, narrow pH ranges (first dimension) and SDS-PAGE (second dimension). Gels were fluorescently stained with ruthenium(II)-tris(bathophenanthrolinedisulfonate).



using WinMDI (Scripps Research Institute). All quantitative data were analyzed by single factor analysis of variance (Microsoft Excel) test for significance (p < 0.05).

RESULTS

Responsiveness of 5L Cells to TCDD

5L cells are highly responsive to AhR/ARNT-mediated gene activation. We have shown previously (37) that exposure of the cells to 1 nm TCDD results in a strong and time-dependent induction of 7-ethoxyresorufin O-deethylase (EROD) activity, an enzymatic activity associated with CYP1A1. In the present study, EROD activity increased from <10 to 1300–1500 pmol of resorufin \times mg of protein⁻¹ \times min⁻¹ within 8 h of treatment (not shown). This exposure period yields about half of the maximal EROD activity that is reached after about 24 h (37).

TCDD-induced Proteome Alterations

Lysates of 5L cells exposed to 1 nm TCDD in Me₂SO or to solvent alone were separated by 2-DE using four different narrow, overlapping 24-cm IPG strips covering a total pH range from 3 to 11 for the IEF step. Following fluorescence staining and quantitative comparison of the gels obtained from treated and untreated cells, gels were silver-stained, and protein spots that had exhibited a statistically significant, reproducible alteration by TCDD were cut out, digested with trypsin, analyzed by MALDI-TOF/TOF mass spectrometry, and identified by database search. Fig. 1 shows representative examples of the fluorescence-stained gels obtained for the four different pH ranges.

With conservative parameter settings for spot detection chosen in such a way that every spot detected by the software was also clearly discernible by visual inspection of the gel images and that, according to our experience, there would be a realistic chance to identify the protein by mass spectrometry, we found a total of \sim 4200 spots that resulted from about 830, 1780, 1070, and 520 spots for the pH ranges 3–5.6, 5.3–6.5, 6.2–7.5, and 7–11, respectively (mean values of eight gels each). Using previously reported Proteomweaver software parameters for spot detection (45), these numbers were increased to \sim 8800 spots that resulted from about 1830, 2790, 2620, and 1570 spots for the respective pH ranges.

The protein species in 78 of the spots with intensities significantly altered by TCDD were identified by mass spectrometry. These protein species, which corresponded to 73 individual proteins, five of which apparently occurred in different posttranslationally modified forms, are listed in Table I.

It is important to note that Table I comprises both proteins with altered abundance, e.g. due to altered expression or half-life, and protein species with altered PTMs. Without further detailed studies, these two types of alterations are difficult or impossible to distinguish. However, as both changes in the abundance of a protein and in the relative proportions of subpopulations of this protein carrying specific PTMs are likely to be functionally relevant, this difficulty does not pose a major problem with regard to the potential biological relevance of the observed alterations.

In Table I, proteins were tentatively categorized according to common functional features. This classification is, however, to a large extent arbitrary because many of these proteins are multitasking proteins playing different roles in different cellular contexts. For the ease of orientation, proteins were consecutively numbered according to the order of their appearance in the table.

MOLECULAR & CELLULAR PROTEOMICS



TABLE I
List of proteins with TCDD-altered abundance

Functional or structural category and protein name ^a	Protein	Swiss-Prot or NCBI accession number	pH range of IPG strip	pl predicted (observed)	Molecular mass predicted (observed)	Regulation factor (TCDD vs. DMSO)	Peptide	Sequence	Protein	Protein score confidence interval
×					Da			%		
Xenobiotic metabolism NOO1	•	P05982	7.0-11.0	8.46	30,853	1.60	19	22	523	100.0
Glutathione S-transferase A2 (GST Ya2) or alutathione	. 2	P04903	7.0–11.0	8,88	25,526	2.16	4	61	302	100.0
S-transferase A3 (GST Yc1)		P04904		8.83	25,229	: i		;		
Glutathione S-transferase P1	За	P04906	6.2-7.5	7.3 (~6–6.2)	23,521	>20	2	34	28	99.4
Glutathione S-transferase P1	36	P04906	5.3-6.5		23,521	4.15	2	က	53	7.76
Aflatoxin B1-aldehyde reductase member 1 (rAFAR1)	4	P38918	6.2-7.5	6.79	37,122	0.62	∞	31	29	6.66
Molecular chaperoning										
60-kDa heat shock protein, mitochondrial precursor (Hsp60)	D O	P19226	5.3-6.5	5.91	61,088	3.48	13	32	170	100.0
neat shock cognate 7 1-kDa protein (neat shock 70-kDa protein 8)	D	010001	0.0-0.0	0.57	000,1	0.43 9.43	20	5	50	0.00
Protein-disulfide isomerase precursor	7	P04785	3 0-5 6	4 82	57.315	1.96	6	41	244	1000
Chanaronin containing TCD1 subunit 9 (8)	- α	54400730	7.0	50.4	57,764	00:0	5 5	- 62	400	0.001
Chaperonin containing TCP1, subunit 2 (p)	ာတ	38969850	5.0.5		61,134	2.00	- o	2 8	154	100.0
Chaperonin containing TCP1, subunit 5 (4)	, C	51260037	30-56	5.51	59,955	0.39	. .	43	179	100.0
Peptidyl-prolyl cis-trans isomerase A	: =	P10111	7.0–11.0	8.37	17.960	0.48	. ∞	i ro	117	100.0
Purine nucleotide biosynthesis					•					
Multifunctional protein ADE2 (includes	12	P51583	6.2-7.5	7.94	47,676	0.65	တ	27	20	100.0
phosphoribosylaminoimidazole-succinocarboxamide										
synthase, phosphoribosyl-aminoimidazole carboxylase)										
Guanine monophosphate synthetase	13	66910916	5.3-6.5	6.21	77,507	1.73	16	31	149	100.0
DNA synthesis and processing										
Replication factor C 2 (40 kDa)	4	55926133	5.3-6.5	6.21	39,031	5.78	∞ ,	က	82	9.66
Minichromosome maintenance protein 7	12	51948378	5.3-6.5	5.90	81,639	1.70	16	38	194	100.0
Heterogeneous nuclear ribonucleoproteins	,		L (i.	0	0	Ó	1	9	
I AK DNA-binding protein (predicted)	9	58865526	5.3-6.5	6.54	32,526	0.00	ກ	27	103	0.001
Amino acid metabolism	1	1	7	0	0	C	7	ć	1	0
Serine hydroxymethyltransferase 2 (mitochondrial)	7.	22/60996	0.11-0.7	8.46	56,243	7.56	21	35	781	0.001
Protein synthesis and processing	Ç	00000	0	0	700	2	1	Ü	7	0
40 S ribosomai protein SA (p40) (34/6/-KDa laminin receptor)	<u>xo</u> (P38983	3.0-0.6	4.80	32,780	2.04	- 1	22	- - - - -	0.001
40 S ribosomal protein S10	19	P63326	7.0–11.0	10.15	18,904	1.54	2	26	24	98.1
60 S acidic ribosomal protein P0 (L10E)	20	P19945	5.3-6.5	5.91	34,365	0.19	9	61	357	100.0
Eukaryotic translation initiation factor 4A, isoform 1	21	4503529	3.0–5.6	5.32	46,353	0.58	∞	25	145	100.0
Eukaryotic translation termination factor 1 (predicted)	22	56605766	5.3-6.5	5.51	49,228	0.62	6	33	86	8.66
Aspartyl-tRNA synthetase Protein phosphorylation	23	P15178	5.3–6.5	6.02	57,546	1.86	23	54	273	100.0
Granine nucleotide-binding protein 3 subunit-like protein	24	P25388	7 0-11 0	7 60	35 511	1 64	22	63	526	1000
12.3 (P205) (receptor of activated protein kinase C 1)	1	2	2	2	- - - - - - - - - - - - - - - - -	5	1	3	2	
Protein dephosphorylation										
Serine/threonine protein phosphatase PP1- α catalytic subunit (PP-1A)	25	P62138	5.3–6.5	5.94	38,229	2.07	Ξ	က	125	100.0
<i></i>										



26 P17220 6.2–7.5 7.12 28 5373347 6.2–7.5 7.02 29 13786144 5.3–6.5 5.29 3 4568084 5.3–6.5 6.15 3 14660688 3.0–5.6 6.15 3 51859482 5.3–6.5 6.18 3 51859482 5.3–6.5 6.18 3 6960688 3.0–5.6 6.18 3 7 908651 5.3–6.5 6.18 3 7 908651 5.3–6.5 6.18 3 91891 7.0–11.0 6.69 3 919559 7.0–11.0 7.44 3 92600851 3.0–5.6 6.57 3 92600851 5.3–6.5 6.25 3 92600851 7.0–11.0 7.44 3 92600851 3.0–5.6 6.57 3 92600851 3.0–5.6 6.57 3 92600851 3.0–5.6 6.33 (6.0–6.1) 3 92600851 3.0–5.6 6.33 (6.0–6.1) 3 927 911883 5.3–6.5 6.33 (6.0–6.1) 3 928 91155 7.0–11.0 7.44 3 91482476 3.0–5.6 5.39 3 92600851 3.0–5.6 5.39 3 92600851 3.0–5.6 6.33 (6.0–6.1) 3 92600851 3.0–5.6 6.33 (6.0–6.1) 3 92600851 3.0–5.6 5.39 3 92600851 3.0–5.6 5.39 3 92600851 3.0–5.6 5.39 3 92600851 3.0–5.6 5.39 3 92600851 3.0–5.6 5.34 (8–5.0) 3 92600851 3.0–5.6 5.31 (48–5.0) 3 92600851 3.0–5.6 5.31 (48–5.0) 3 92600851 3.0–5.6 5.31 (48–5.0) 3 92600851 3.0–5.6 5.31 (48–5.0) 3 92600851 3.0–5.6 5.31 (48–5.0) 3 92600851 3.0–5.6 5.31 (48–5.0)	or NCBI primary pl predicted accession strip (observed) number	mass predicted (observed)	Regulation factor (TCDD vs. DMSO)	Peptide count	Sequence coverage	Protein score	Protein score confidence interval
t 12 27 27 28 53733547 6.2-7.5 5.29 14786144 5.3-6.5 5.29 14786144 5.3-6.5 5.59 14386144 5.3-6.5 5.59 14386144 5.3-6.5 5.59 14386144 5.3-6.5 5.59 14386144 5.3-6.5 5.43 140 131 56606883 3.0-5.6 5.11 11 12 12 132 132 132 132 132 132 132		Da			%		
t 12 2	1 1 0	i d	0	1	ć	ć	1
total transfer of the protein I (UQCRC1)	6.2–7.5	25,893	2.38	_ 0	23 1	62	99.7
trd2 28 53/3344 6.2-7.5 7.02 29 13786144 5.3-6.5 5.59 30 47866184 5.3-6.5 5.59 31 56605688 3.0-5.6 5.11 32 P35559 5.3-6.5 6.18 33 51859482 5.3-6.5 6.18 34 008651 5.3-6.5 6.18 37 008651 5.3-6.5 6.28 38 09EQS0 7.0-11.0 6.69 Precursor 36 P52873 5.3-6.5 6.25 Precursor 37 P04636 7.0-11.0 7.44 39b P81155 7.0-11.0 7.44 39b P81155 7.0-11.0 7.44 39b P81155 7.0-11.0 7.44 42a P11883 5.3-6.5 6.33 (6.0-6.1) kr1b8 protein) 40 51948476 3.0-5.6 5.33 (6.0-6.1) 42b P11883 5.3-6.5 6.33 (6.0-6.1) 47 P07632 5.3-6.5 5.89 cytoplasmic 45 P17425 5.3-6.5 5.88 49 P07632 5.3-6.5 6.08 49 P07632 5.3-6.5 6.25 5.00 P60259 3.0-5.6 5.31 (4.8-5.0) 60 P60271 5.3-6.5 6.31 (4.8-5.0)	3.0-5.6	28,498	0.65	∞ (35	96	0.001
ted) 31 45680894 5.3-6.5 5.59 ted) 32 45680894 5.3-6.5 5.59 tease) 33 51859482 5.3-6.5 6.18 and kinase, MZ isozyme 34 O08651 5.3-6.5 6.28 precursor 35 P3559 7.0-11.0 6.69 precursor 38 Q9EQS0 6.2-7.5 6.27 precursor 42 P11883 5.3-6.5 6.33 (6.0-6.1) kr1b8 protein) 42 P17425 5.3-6.5 6.33 (6.0-6.1) kr1b8 protein) 44 P07632 5.3-6.5 6.33 (6.0-6.1) kr1b8 protein) 45 P17425 5.3-6.5 6.25 convertase) (ICE) 46 P43527 6.2-7.5 6.25 57 C0-11.0 7.44 P07632 5.3-6.5 6.33 (6.0-6.1) 48 P10760 5.3-6.5 6.38 49 202549 3.0-5.6 5.31 (4.8-5.0) pe0711 50a P63259 3.0-5.6 5.31 (4.8-5.0)	6.2–7.5	53,302	0.52	16	21	164	100.0
ted) 31 45680894 5.3-6.5 5.43 ted) 32 P35559 5.3-6.5 6.18 trase) 33 51859482 5.3-6.5 6.18 trate kinase, M2 isozyme 35 P11980 7.0-11.0 6.69 precursor 36 P52873 5.3-6.5 6.25 precursor 37 P04636 7.0-11.0 6.69 precursor 37 P04636 7.0-11.0 7.44 precursor 41 P10719 3.0-5.6 5.57 precursor 42 P11883 5.3-6.5 6.33 (6.0-6.1) kr1b8 protein) 40 51948476 3.0-5.6 5.38 cytoplasmic 45 P17425 5.3-6.5 6.25 precursor 45 P17425 5.3-6.5 6.25 convertase) (ICE) 46 P43527 6.2-7.5 6.25 sonvertase) (ICE) 46 P43527 6.2-7.5 6.25 transfer 47 P30349 5.3-6.5 5.36 transfer 48 P10760 5.3-6.5 5.31 (4.8-5.0) transfer 49 P60711 5.0a P63259 3.0-5.6 5.31 (4.8-5.0) transfer 49 P60711 5.0a P63259 3.0-5.6 5.31 (4.8-5.0)	5.3-6.5	81,659	0.44	9	31	332	100.0
ted) 31 56605688 3.0-5.6 5.11 erase) 32 P35559 5.3-6.5 6.18 ate kinase, M2 isozyme 35 P11980 7.0-11.0 6.69 precursor 36 P52873 5.3-6.5 6.28 precursor 37 P04636 7.0-11.0 7.44 are protein I (UQCRC1) 40 51948476 3.0-5.6 5.37 precursor 42 P11883 5.3-6.5 6.33 (6.0-6.1) kr1b8 protein) 43 51480424 6.2-7.5 6.33 cytoplasmic 45 P17425 5.3-6.5 5.89 cytoplasmic 45 P17425 5.3-6.5 6.08 48 P10760 5.3-6.5 6.08 49 202549 3.0-5.6 5.31 (4.8-5.0) erase) are kinase, M2 isozyme 35 1480424 6.2-7.5 6.37 are protein I (UQCRC1) 40 51948476 3.0-5.6 6.33 are protein I (UQCRC1) 40 51948476 3.0-5.6 6.08 are protein I (UQCRC1) 40 51948476 3.0-5.6 5.31 (4.8-5.0) are protein I (UQCRC1) 40 6.3-6.5 6.33 (6.0-6.1) brownertase) (ICE) 46 P43527 6.2-7.5 6.25 are protein I (B-actin) 50a P63259 3.0-5.6 5.31 (4.8-5.0) are protein I (B-actin) 60a P63259 3.0-5.6 5.31 (4.8-5.0)	5.3–6.5	53,116	1.66	တ ု	25	128	100.0
erase) 32 P35599 5.3-6.5 6.18 33 008651 5.3-6.5 6.28 74e kinase, M2 isozyme 35 P11980 7.0-11.0 6.69 740 P11981 7.0-11.0 6.69 740 P11981 7.0-11.0 8.92 740 P81155 7.0-11.0 7.44 39b P81155 7.0-11.0 7.44 39b P81155 7.0-11.0 7.44 39b P81155 7.0-11.0 7.44 39b P81155 7.0-11.0 7.44 40 51948476 3.0-5.6 6.33 42a P11883 5.3-6.5 6.33 (6.0-6.1) 42a P11883 5.3-6.5 6.33 (6.0-6.1) 44 P07632 5.3-6.5 6.33 59b P11883 5.3-6.5 6.35 cytoplasmic 45 P17425 5.3-6.5 5.89 cytoplasmic 1(β-actin) 50a P63259 3.0-5.6 5.31 (4.8-5.0) P60711 5.29 (4.8-5.0)	3.0–5.6	56,397	0.54	<u>5</u>	36	97	100.0
erase) 33 51859482 5.3-6.5 6.18 34 008651 5.3-6.5 6.28 7.0-11.0 6.69 7.0-11.0 6.69 7.0-11.0 6.69 7.0-11.0 6.69 7.0-11.0 6.69 7.0-11.0 6.69 7.0-11.0 6.69 7.0-11.0 7.44 7.40 7.40 7.40 7.40 7.40 7.40 7.41 7.41 7.41 7.41 7.42 7.41 7.42 7.44 7.4	5.3–6.5	118,376	3.43	12	12	99	99.0
state kinase, M2 isozyme 35 P11980 7.0–11.0 6.689 7.40 7.40 7.40 7.40 7.40 7.40 7.40 7.40	5.3-6.5	38,097	5.78	10	36	149	100.0
sylvate kinase, M2 isozyme 35 P11980 7.0–11.0 6.69 precursor 36 P52873 5.3–6.5 6.26 17.40 precursor 37 P04636 7.0–11.0 8.92 precursor 38 Q9EQS0 6.2–7.5 6.57 precursor 42 P81155 7.0–11.0 7.44 precursor 42 P11883 5.3–6.5 6.33 (6.0–6.1) kr1b8 protein) 43 51480424 6.2–7.5 8.58 cytoplasmic 45 P17425 5.3–6.5 5.89 cytoplasmic 7 (β-actin) 50a P63259 3.0–5.6 5.31 (4.8–5.0) precursor 48 P10760 5.3–6.5 6.25 cytoplasmic 1 (β-actin) 50a P63259 3.0–5.6 5.31 (4.8–5.0) precursor 48 P60711 5.29 (4.8–5.0)							
rate kinase, MZ Isozyme 35 P11980 7.0–11.0 6.69 precursor 36 P52873 5.3–6.5 6.25 17 precursor 37 P04636 7.0–11.0 7.44 39a P81155 7.0–11.0 7.44 39b P81155 7.0–11.0 7.44 40 51948476 3.0–5.6 5.57 precursor 42a P11883 5.3–6.5 6.33 (6.0–6.1) kr1b8 protein) 43 51480424 6.2–7.5 8.58 cytoplasmic (ICE) 46 P43527 6.2–7.5 6.25 convertase) (ICE) 46 P43527 6.2–7.5 6.25 cytoplasmic 1 (β-actin) 50a P63259 3.0–5.6 5.31 (4.8–5.0) precursor 7.40 49 202549 3.0–5.6 5.31 (4.8–5.0) p60711 5.29 (4.8–5.0)	5.3-6.5	57,256	1.76	16	31	252	100.0
precursor 36 P52873 5.3-6.5 6.25 1 precursor 37 P04636 7.0-11.0 8.92 38 Q9EQSO 6.2-7.5 6.57 specursor 40 51948476 3.0-5.6 5.19 precursor 41 P10719 3.0-5.6 5.19 kr1b8 protein) 42a P11883 5.3-6.5 6.33 kr1b8 protein) 42b P11883 5.3-6.5 6.33 cytoplasmic 45 P17425 5.3-6.5 5.89 convertase) (ICE) 46 P43527 6.2-7.5 6.25 cytoplasmic 47 P30349 5.3-6.5 6.08 48 P10760 5.3-6.5 6.08 49 202549 3.0-5.6 5.31 (4.8-5.0) 609 5.39 (4.8-5.0)	0.11-0./	58,163 58.183	0.00	35	2/	0/9	0.001
recursor 36 P52873 5.3-6.5 6.25 1 precursor 37 P04636 7.0-11.0 8.92 1 specursor 39a P81155 7.0-11.0 7.44 re protein I (UQCRC1) 40 51948476 3.0-5.6 5.57 precursor 41 P10719 3.0-5.6 5.19 kr1b8 protein) 42b P11883 5.3-6.5 6.33 kr1b8 protein) 42b P11883 5.3-6.5 6.33 cytoplasmic 45 P17425 5.3-6.5 5.89 cytoplasmic 45 P17425 5.3-6.5 5.58 convertase) (ICE) 46 P43527 6.2-7.5 6.25 47 P30349 5.3-6.5 6.08 48 P10760 5.3-6.5 6.08 49 202549 3.0-5.6 5.31 (4.8-5.0) 5.99 (4.8-5.0) 9.0-5.6 5.31 (4.8-5.0)							
precursor 37 P04636 7.0–11.0 8.92 38 Q9EQSO 6.2–7.5 6.57 39a P81155 7.0–11.0 7.44 we protein I (UQCRC1) 40 51948476 3.0–5.6 5.57 precursor 42a P11883 5.3–6.5 6.33 (6.0–6.1) 42b P11883 5.3–6.5 6.38 (6.0–6.1) 44 P07632 5.3–6.5 6.28 convertase) (ICE) 46 P43527 6.2–7.5 6.25 51965 5.70 48 P10760 5.3–6.5 6.08 49 202549 3.0–5.6 5.31 (4.8–5.0) P60711 50a P63259 3.0–5.6 5.29 (4.8–5.0)	5.3-6.5	130,349	2.46	27	က	224	100.0
39a P81155 7.0–11.0 7.44 39b P81155 7.0–11.0 7.44 re protein I (UQCRC1) 40 51948476 3.0–5.6 5.19 precursor 42a P11883 5.3–6.5 6.33 (6.0–6.1) kr1b8 protein) 43 51480424 6.2–7.5 8.58 cytoplasmic 45 P17425 5.3–6.5 6.25 convertase) (ICE) 46 P43527 6.2–7.5 6.25 convertase) (ICE) 47 P30349 5.3–6.5 6.08 48 P10760 5.3–6.5 6.08 49 P63259 3.0–5.6 5.31 (4.8–5.0) P60711 50a P63259 3.0–5.6 5.30 (4.8–5.0)	7.0–11.0	36,089	>20	20	63	646	100.0
39a P81155 7.0–11.0 7.44 39b P81155 7.0–11.0 7.44 39b P81155 7.0–11.0 7.44 39b P81155 7.0–11.0 7.44 42a P11883 5.3–6.5 6.33 (6.0–6.1) 42b P11883 5.3–6.5 6.33 (6.0–6.1) 44 P07632 5.3–6.5 6.38 (6.0–6.1) 45 P17425 5.3–6.5 6.25 50nvertase) (ICE) 46 P43527 6.2–7.5 6.25 48 P10760 5.3–6.5 6.08 49 202549 3.0–5.6 5.31 (4.8–5.0) P60711 50a P63259 3.0–5.6 5.31 (4.8–5.0)							
39a P81155 7.0–11.0 7.44 re protein I (UQCRC1) 40 51948476 3.0–5.6 5.57 precursor 42a P11883 5.3–6.5 6.33 kr1b8 protein) 43 51480424 6.2–7.5 8.58 cytoplasmic 45 P17425 5.3–6.5 5.38 convertase) (ICE) 46 P43527 6.2–7.5 6.25 convertase) (ICE) 47 P30349 5.3–6.5 5.70 48 P10760 5.3–6.5 6.08 48 P10760 5.3–6.5 6.08 49 202549 3.0–5.6 6.08 49 P63259 3.0–5.6 5.31 (4.8–5.0)	6.2-7.5	37,624	1.57	တ	က	102	100.0
39a P81155 7.0–11.0 7.44 39b P81155 7.0–11.0 7.44 re protein I (UQCRC1) 40 51948476 3.0–5.6 5.57 precursor 42a P11883 5.3–6.5 6.33 (6.0–6.1) 42b P11883 5.3–6.5 6.33 (6.0–6.1) 44 P07632 5.3–6.5 6.38 (6.0–6.1) 45 P17425 5.3–6.5 6.25 convertase) (ICE) 46 P43527 6.2–7.5 6.25 47 P30349 5.3–6.5 6.08 48 P10760 5.3–6.5 6.08 49 202549 3.0–5.6 5.31 (4.8–5.0) P60711 5.29 (4.8–5.0)							
re protein I (UQCRC1) 40 51948476 3.0–5.6 5.57 precursor 41 P10719 3.0–5.6 5.19 kr1b8 protein) 42a P11883 5.3–6.5 6.33 6.0–6.1 kr1b8 protein) 43 51480424 6.2–7.5 8.58 cytoplasmic 45 P17425 5.3–6.5 5.89 convertase) (ICE) 46 P43527 6.2–7.5 6.25 convertase) (ICE) 46 P43527 6.2–7.5 6.25 47 P30349 5.3–6.5 5.70 48 P10760 5.3–6.5 6.08 49 202549 3.0–5.6 5.31 (4.8–5.0) P60711 5.29 (4.8–5.0)	7.0–11.0	32,353	2.11	7	က	124	100.0
re protein I (UQCRC1) 40 51948476 3.0–5.6 5.57 precursor 42a P11883 5.3–6.5 6.33 (6.0–6.1) 42b P11883 5.3–6.5 6.33 (6.0–6.1) 44 P07632 5.3–6.5 5.89 cytoplasmic 45 P17425 5.3–6.5 5.89 convertase) (ICE) 46 P43527 6.2–7.5 6.25 convertase) (ICE) 47 P30349 5.3–6.5 6.08 48 P10760 5.3–6.5 6.08 49 P03259 3.0–5.6 5.31 (4.8–5.0) P60711 5.29 (4.8–5.0)	7.0–11.0	32,353	0.02	-	9	22	98.1
re protein I (UQCRC1)							
precursor 41 P10719 3.0–5.6 5.19 42a P11883 5.3–6.5 6.33 (6.0–6.1) 42b P11883 5.3–6.5 6.33 (6.0–6.1) 43 51480424 6.2–7.5 8.58 cytoplasmic 45 P17425 5.3–6.5 5.89 convertase) (ICE) 46 P43527 6.2–7.5 6.25 47 P30349 5.3–6.5 5.70 48 P10760 5.3–6.5 6.08 49 202549 3.0–5.6 5.31 (4.8–5.0) P60711 5.29 (4.8–5.0)	3.0–5.6	53,500	0.63	တ	24	109	100.0
kr1b8 protein) 42a P11883 5.3-6.5 6.33 (6.0-6.1) kr1b8 protein) 43 51480424 6.2-7.5 8.58 cytoplasmic 45 P17425 5.3-6.5 5.89 convertase) (ICE) 46 P43527 6.2-7.5 6.25 47 P30349 5.3-6.5 5.70 5.3-6.5 6.08 48 P10760 5.3-6.5 6.08 49 202549 3.0-5.6 5.31 (4.8-5.0) 49 P63259 3.0-5.6 5.31 (4.8-5.0)	3.0–5.6	56,318	1.97	-	31	131	100.0
kr1b8 protein) 42a P11883 5.3-6.5 6.33 kr1b8 protein) 43 51480424 6.2-7.5 8.58 cytoplasmic 45 P17425 5.3-6.5 5.89 convertase) (ICE) 46 P43527 6.2-7.5 6.25 47 P30349 5.3-6.5 5.70 48 P10760 5.3-6.5 6.08 49 202549 3.0-5.6 4.87 ycytoplasmic 1 (β-actin) 50a P63259 3.0-5.6 5.31 (4.8-5.0) P60711 5.29 (4.8-5.0)	1	1		;	!	į	
kr1b8 protein) 42b P11883 5.3-6.5 6.33 (6.0-6.1) 43 51480424 6.2-7.5 8.58 44 P07632 5.3-6.5 5.89 cytoplasmic 45 P17425 5.3-6.5 5.58 convertase) (ICE) 46 P43527 6.2-7.5 6.25 47 P30349 5.3-6.5 5.70 48 P10760 5.3-6.5 6.08 49 202549 3.0-5.6 4.87 49 202549 3.0-5.6 5.31 (4.8-5.0) P60711 5.29 (4.8-5.0)	5.3-6.5		2.20	25	43	473	100.0
kr1b8 protein) 43 51480424 6.2–7.5 8.58 cytoplasmic 1 (β-actin) 44 P07632 5.3–6.5 5.89 cytoplasmic 1 (β-actin) 50a P63259 3.0–5.6 5.31 (4.8–5.0) P60711 5.29 (4.8–5.0)	5.3–6.5		1.81	24	56	531	100.0
cytoplasmic 1 (β-actin) 50a P63259 5.3–6.5 5.89 cytoplasmic 1 (β-actin) 50a P63259 3.0–5.6 5.31 (4.8–5.0)	6.2–7.5	34,891	0.50	9	41	104	100.0
cytoplasmic 45 P17425 5.3-6.5 5.58 convertase) (ICE) 46 P43527 6.2-7.5 6.25 47 P30349 5.3-6.5 5.70 48 P10760 5.3-6.5 6.08 49 202549 3.0-5.6 4.87 49 P63259 3.0-5.6 5.31 (4.8-5.0) P60711 5.29 (4.8-5.0)	5.3-6.5	15,942	0.65	n	54	132	0.001
convertase) (ICE) 46 P43527 6.2–7.5 6.25 5.70 48 P10760 5.3–6.5 6.08 4.87 49 202549 3.0–5.6 5.31 (4.8–5.0) P60711 5.29 (4.8–5.0)	с с ц	78 025		7	90	171	1000
convertase) (ICE) 46 P43527 6.2-7.5 6.25 47 P30349 5.3-6.5 5.70 48 P10760 5.3-6.5 6.08 49 202549 3.0-5.6 4.87 49 P63259 3.0-5.6 5.31 (4.8-5.0) P60711 5.29 (4.8-5.0)		0,00	9	2	2	<u>-</u>	2
47 P30349 5.3–6.5 5.70 48 P10760 5.3–6.5 6.08 49 202549 3.0–5.6 4.87 tin, cytoplasmic 1 (β-actin) 50a P63259 3.0–5.6 5.31 (4.8–5.0) P60711 5.29 (4.8–5.0)	6.2-7.5	46.173	1.57	12	16	25	98.5
48 P10760 5.3-6.5 6.08 49 202549 3.0-5.6 4.87 tin, cytoplasmic 1 (β -actin) 50a P63259 3.0-5.6 5.31 (4.8-5.0) P60711 5.29 (4.8-5.0)	5.3-6.5	69,628	1.57	, 1	့ က	188	100.0
48 P10760 5.3–6.5 6.08 49 202549 3.0–5.6 4.87 tin, cytoplasmic 1 (β -actin) 50a P63259 3.0–5.6 5.31 (4.8–5.0) P60711 5.29 (4.8–5.0)							
49 202549 3.0–5.6 4.87 tin, cytoplasmic 1 (β -actin) 50a P63259 3.0–5.6 5.31 (4.8–5.0) P60711 5.29 (4.8–5.0)	5.3-6.5	47,889	1.69	12	25	66	100.0
49 202549 3.0–5.6 4.87 tin, cytoplasmic 1 (β -actin) 50a P63259 3.0–5.6 5.31 (4.8–5.0) P60711 5.29 (4.8–5.0)							
tin, cytoplasmic 1 (β -actin) 50a P63259 3.0–5.6 5.31 (4.8–5.0) P60711 5.29 (4.8–5.0)	3.0-5.6	54,375	1.96	19	44	183	100.0
or actin, cytoplasmic 1 (β -actin) 50a P63259 3.0–5.6 5.31 (4.8 –5.0) P60711 5.29 (4.8 –5.0)							
P60711 5.29 (4.8–5.0)	3.0–5.6 5.31		2.48	2	42	405	100.0
(C L L L C C L C C C C C C C C C C C C C	5.29		,	(ć	1	0
Actin, cytopiasmic 2 (γ-actin) 500 P63259 5.3-6.5 5.31 (5.5-5.6) 42,108	5.3-6.5 5.31		02.<	٥	23	115	100.0

d
9
ž
5
₽
2
Ö
O
-
111
BLE
ø
,<

Functional or structural category and protein name ^a	Protein	Swiss-Prot or NCBI accession number	pH range of IPG strip	pl predicted (observed)	Molecular mass predicted (observed)	Regulation factor (TCDD vs. DMSO)	Peptide	Peptide Sequence Protein count coverage score		Protein score confidence interval
Capping protein (actin filament), gelsolin-like (predicted)	51	61556900	5.3-6.5	6.11	<i>Da</i> 39,060	1.58	12	% 49	195	100.0
Calponin-3	52	P37397	3.0–5.6	5.47	36,583	1.66	9		54	98.4
Septin 2	53	16924010	5.3-6.5	6.15	41.737	1.58	16	49	206	100.0
Annexin A1	5.54	P07150	6.2-7.5	7.14	39.016	>>0	<u>></u>	2 %	8 6	100.0
Annexin A6	55	P48037	5.3-6.5	5.39	75.975	0.30	23	33	216	100.0
Drebrin	26	007266	3.0-5.6	4.46	78.223	0.49	15	27	142	100.0
Myosin regulatory light chain 2-A, smooth muscle	57a	P13832	3.0–5.6	4.67 (3.2–3.4)	19,80919,752	0.58	00	63	295	100.0
isoform or myosin regulatory light chain 2-B, smooth muscle isoform		P18666		4.78 (3.2–3.4)						
Myosin regulatory light chain 2-A, smooth muscle	57b	P13832	3.0-5.6	4.67 (3.3–3.5)	19,809 (17-18 kDa)	0.62	10	99	368	100.0
isoform or myosin regulatory light chain 2-B, smooth muscle isoform		P18666		4.78 (3.3–3.5)	19,752 (17–18 kDa)					
Tropomyosin $\alpha 4$ chain (tropomyosin 4) or tropomyosin β chain (tropomyosin β)	28	P09495 P58775	3.0–5.6	4.66	28,549	>20	19	94	260	100.0
	50	P30427	3 0-5	5 71 (4 9-5 1)	535 152	0.45	23	7	43	080
Vimentin	8 6	P31000	9.00 10.00 10.00 10.00	5.06	53 626	20.5	000	, K	457	100.0
I min A	8 6	P48679	2 C	6.54	74.564	1 71	2 6	8 8	280	1000
Tubulin 8-5 chain	62	P05218	3.0-5.6	4.78	50,095	>20	7	36	172	100.0
Miscellaneous	!			•		ì		}		
14-3-3 protein τ (14-3-3 protein θ)	63	P35216	3.0-5.6	4.69	28,046	0.62	17	99	297	100.0
14-3-3 protein \$\inf\$ (protein kinase C inhibitor protein-1) (KCIP-1) (mitochondrial import stimulation factor	64	P35216	3.0–5.6	4.73	27,925	0.61	21	75	528	100.0
Complement component 1, Q subcomponent-binding	65	035796	3.0–5.6	4.81	31,006	0.63	2	27	100	100.0
protein, mitochondrial precursor	Ċ	0000	(L	000	1	,	Ċ	9	0
WD repeat domain 1		62078997	5.3-6.5	6.15	66,824	1.69	16	36	182	100.0
Predicted: similar to purine-nucleoside phosphorylase		34869683	5.3-6.5	6.46	32,566	1.55	ი ·	36	105	100.0
Predicted: similar to esterase D/formylglutathione	89	62661724	5.3-6.5	6.45	37,322	1.65	4	16	100	100.0
	ć	7	(1	7	0	c	1	7	
Predicted: similar to dendritic cell protein GA1/	9 6	62645491	5.3-6.5	5.70	64,714	0.37	ກ (<u>/</u> L	27.5	0.001
riedicted, similar to vincuiii (metavincuiii)) - 	02001011	0.010.0	0.20	103,230	2.02	00 :	2 :	744	0.00
Predicted: similar to septin 11	71	109499524	5.3-6.5	8.56 (6.3–6.4)	969'59	1.60	9	18	267	100.0
Predicted: similar to capping protein (actin filament)	72	62644141	5.3-6.5	5.43	33,060	1.73	5	63	168	100.0
Predicted: similar to α -glucosidase II, α subunit	73	62641851	5.3-6.5	5.76	109,846	1.75	33	45	273	100.0
^a Protein entries occurring twice represent different forms of the same protein present in distinct protein spots.	rms of th	e same protei	n present in	distinct proteir	spots.					

Known and Putative New Members of the AhR and ARE Gene Batteries - Among the proteins identified as up-regulated by TCDD were several well known members of the AhR and ARE gene batteries, namely aldehyde dehydrogenase 3A1 (ALDH3A1, number 42), NAD(P)H:quinone oxidoreductase 1 (NQO1, number 1), and, most likely, glutathione S-transferase A2 (GSTA2, formerly called Ya2) (number 2). GSTA2 was identified in an up-regulated protein spot that may have also contained another class Alpha GST isoenzyme, GSTA3 (formerly Yc1) because no peptides unique to GSTA2 as compared with GSTA3 (and vice versa) were identified (see supplemental Table S1). Although it appears likely that GSTA2 induction was involved in the up-regulation of the GST protein spot, a contribution of GSTA3 cannot be ruled out as in our previous study (37) we had observed a significant up-regulation of peptides characteristic for both GSTA3 and GSTA5 (formerly Yc2). As the rat GSTA5 gene contains an AHRE-I within the first intron that is active in regulating transcription (46), an induction of this GST isoform, which has also been detected as up-regulated in a recent microarray analysis on gene expression in TCDD-treated rats (19), by TCDD would also appear plausible.

In addition to the induction of GSTA2 (or, possibly, GSTA3), we detected an induction of GSTP1 (number 3). GSTP1 was identified in two individual up-regulated protein spots (numbers 3a and 3b) of apparently the same molecular weight but with different pl values that probably represented distinct individual forms of the enzyme carrying different PTMs.

The proteins with increased abundance following TCDD treatment also included several for which there is evidence from other experimental systems that their induction may be controlled via the ARE. These proteins were insulin-degrading enzyme (number 32), transaldolase (number 38), lamin A (number 62), and tubulin β -5 chain (number 63), which were recently identified as regulated in an ARE-dependent manner in mice (47, 48). To the best of our knowledge, they have not been known previously to be affected by TCDD. Moreover we observed that two subunits (β and γ , numbers 8 and 9) of the chaperonin containing t-complex polypeptide 1 (chaperonin containing TCP1 (CCT)) were up-regulated by TCDD. As the expression of the η subunit of CCT has been reported to be regulated via the ARE in mouse liver (47) and as it appears likely that the expression of the multiple chaperonin subunits occurs coordinately, it seems possible that the observed upregulation of the β and γ subunits also depends on an AREmediated mechanism.

We also observed that TCDD affected the enzyme aflatoxin B1-aldehyde reductase (AFAR1 or AKR7A1) (number 4) in 5L cells. The AFAR1 gene contains numerous ARE-related sequences and also one AHRE-I in its promoter region (49) and thus might be expected to be up-regulated by TCDD. However, we did not observe an up-regulation but a significant down-regulation of an AFAR1 species. Thus, further work is clearly required to characterize the effects of TCDD on the level and PTMs of AFAR1 protein in 5L cells.

Cytoskeletal Proteins - A large group of proteins with altered abundance or PTMs was comprised of structural proteins. Thus, in addition to several proteins of or associated with the cytoskeleton that we recently identified as altered by TCDD (37) and that recurred in the present study (numbers 50 and 57-60), we observed quantitative changes of protein spots corresponding to several actin-interacting proteins (50) not previously known to be affected by TCDD. They include capping protein (number 51), calponin-3 (number 52), the GTPase septin 2 (number 53), drebrin (number 56), and tubulin β -5 chain (number 62). These alterations coincide with the up-regulation of two subunits of CCT (numbers 8 and 9), a cytosolic molecular chaperone composed of eight subunits that assists in the folding of actin and tubulin and other cytosolic proteins (51). The data support the notion (37) that TCDD exposure results in a highly complex, coordinated reorganization of the cytoskeleton of 5L cells.

Proteins Involved in the Maintenance of Mitochondrial Homeostasis—Several findings of the present study strongly support our previous observation of a marked effect of TCDD on mitochondrial homeostasis (37). Thus, we observed significant alterations of two components of the respiratory chain, namely a down-regulation of ubiquinol-cytochrome c reductase core protein I (UQCRC1, number 40), a core subunit of mitochondrial respiratory complex III, and an up-regulation of the β chain of the mitochondrial ATP synthase (number 41). Up-regulation of the latter is a characteristic cellular response to certain toxicants that has been attributed to an adaptation of cells to mitochondrial damage induced by ROS (52, 53).

An intriguing finding with regard to the response of mitochondria to dioxin exposure was the observation that TCDD clearly affected the appearance of the voltage-dependent anion channel-selective protein 2 (VDAC2) in 5L cells. VDAC2 functions as a pore in the outer mitochondrial membrane by mediating metabolic exchange between mitochondria and the cytoplasm and acts as a key regulator of mitochondrial BAK-mediated apoptosis (54, 55).

TCDD treatment for 8 h altered the intensities of two closely spaced protein spots, both of which were subsequently identified as VDAC2 (Table I, number 39, and Fig. 2A). Whereas the more acidic spot VDAC2b disappeared almost completely in the TCDD-treated cells, the intensity of its more basic counterpart, VDAC2a, increased by a factor of \sim 2.1 (Fig. 2B). Because a TCDD-induced increase in the abundance of VDAC2 would potentially have important consequences for the regulation of apoptosis in 5L cells, we monitored the abundance of VDAC2 protein by Western blotting over treatment periods of up to 24 h. TCDD treatment clearly caused a marked and time-dependent induction of total VDAC2 protein (Fig. 2C), indicating that the observed increase in VDAC2a was not merely the consequence of a conversion of the more acidic to the more basic VDAC2 form. Thus, it appears that TCDD exposure results in both an altered PTM of VDAC2 and an increase in its abundance.

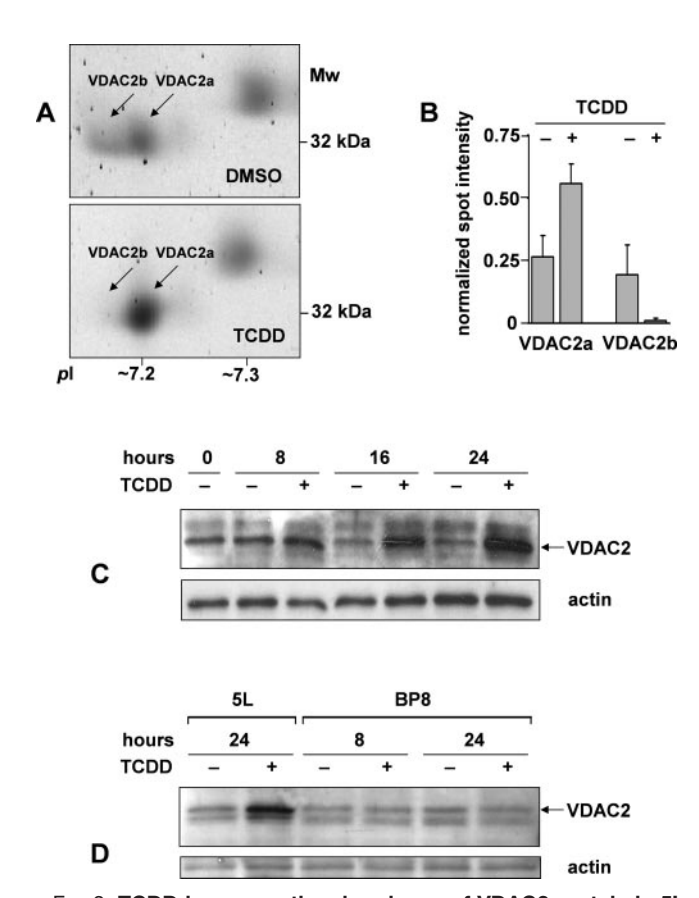


Fig. 2. TCDD increases the abundance of VDAC2 protein in 5L cells but not in AhR-deficient BP8 cells. Cells were exposed to Me₂SO or 1 nm TCDD for 8 h (A and B) or the times indicated (C and D) and analyzed by 2-DE and fluorescence staining (A and B) or one-dimensional Western blotting (C and D) using anti-VDAC2 and anti-actin antibodies. A, sections of two representative 2D gels (pH range 7-11) showing the up-regulation of VDAC2. On the horizontal axis, pl values, as estimated from the pH profile of the non-linear gradient, are indicated. On the vertical axis, molecular masses, as estimated from molecular weight markers, are given. VDAC2 is indicated by arrows. B, statistical analysis of VDAC2 up-regulation. Bars represent the means ± S.D. from groups of four individual gels. C, Western blot analysis of VDAC2 protein abundance in 5L cells treated with Me₂SO or 1 nm TCDD for the times indicated. The actin band served as loading control. D, Western blot analysis of VDAC2 protein abundance in BP8 cells treated with Me₂SO or 1 nm TCDD for 8 and 24 h. 5L cells served as positive control; the actin band served as loading control. C and D each represent sections of blots from one experiment of three to five experiments that yielded very similar results.

TCDD did not induce VDAC2 protein in BP8 cells, an AhR-deficient subline of the 5L cells (29) (Fig. 2D), indicating that up-regulation is dependent on the presence of a functional AhR. To determine whether the increase in the abundance of VDAC2 protein was accompanied by a stimulation of VDAC2 expression at the transcriptional level, we performed real time PCR analyses. The obtained results showed that the abundance of VDAC2 mRNA was not detectably affected by TCDD over an incubation period of up to 24 h, whereas the mRNA level of CYP1A1, which served as a positive control, increased

several hundredfold within 24 h (not shown). These results indicate that the up-regulation of VDAC2 occurs at the translational level or via an increase in protein half-life.

TCDD-induced Oxidative Stress

Transcription of ARE-regulated genes can be activated by both electrophiles and oxidants (56–58). As TCDD does not yield electrophilic metabolites, it appeared possible that the observed increases in the abundance of proteins with ARE-containing gene promoters occurred in response to TCDD-induced oxidative stress. To determine whether TCDD treatment actually induces oxidative stress in 5L cells, we used the redox-active probe DHR123. Cells were treated with 1 nm TCDD in Me₂SO or only Me₂SO for 8 h and then loaded with DHR123. This compound, an uncharged and nonfluorescent dye, passively diffuses across cell membranes and reacts with ROS, resulting in the formation of cationic fluorescent R123 that can be quantitated by flow cytometry.

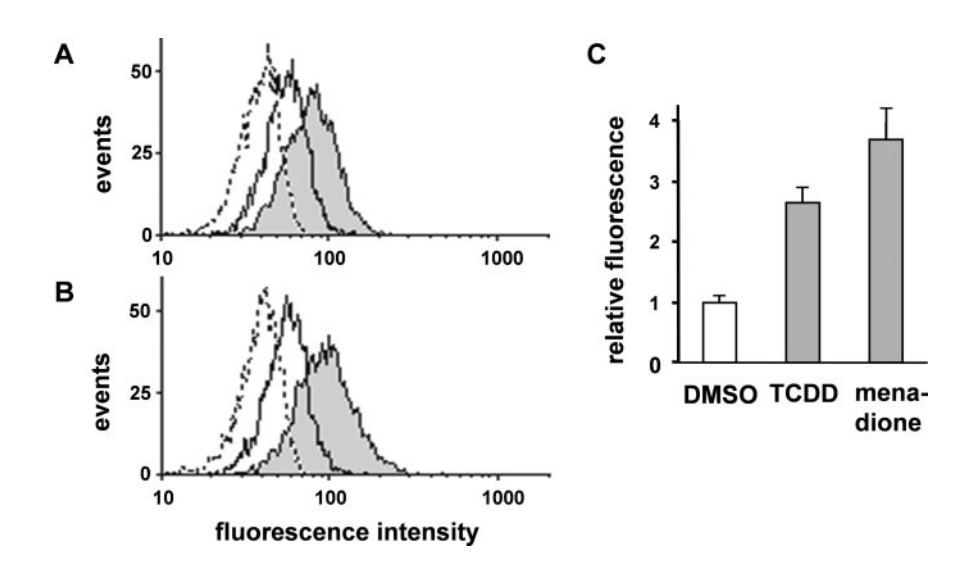
Fig. 3A shows that the mean R123 fluorescence in TCDD-treated cells increased by about 165% as compared with that of the ${\rm Me_2SO}$ -treated control. Treatment of the cells with 50 $\mu{\rm M}$ menadione (2-methyl-1,4-naphthoquinone), which produces reactive oxygen species by redox cycling and which was used as a positive control, for 30 min increased R123 fluorescence by about 265% (Fig. 3B). These results show that TCDD treatment in fact results in the production of ROS in 5L cells.

DISCUSSION

The present study was conducted as part of an effort to provide a better understanding of the effects of TCCD on hepatic cells. The rat hepatoma cell line 5L, one of the rather limited number of established liver cell lines showing overt signs of toxicity in response to TCDD, was used as an *in vitro* model. In 5L cells, dioxin toxicity manifests itself primarily by an inhibition of cell proliferation and, eventually, initiation of apoptotic death. Several previous investigations have addressed specific aspects of the toxicity of TCDD in 5L cells. Until lately, global, non-hypothesis-driven approaches with the potential to uncover novel, unanticipated aspects of dioxin action in 5L cells have been limited to a transcriptomics analysis that gave rise to the discovery of the regulatability of the expression of the *N*-myristoyltransferase 2 gene (14).

In a quantitative proteomics study on the effects of TCDD on the proteins of 5L cells using the ICPL method we have recently identified a large number of proteins with altered abundance or PTMs upon exposure of the cells to the dioxin (37). The majority of these alterations had not been known before. In view of the large number of up- or down-regulated protein species detected we reckoned that an independent, technically unrelated approach for proteome analysis would presumably identify an additional, different set of TCCD-responsive proteins that might give further clues to the largely

Fig. 3. TCDD induces ROS formation in 5L cells. Cells were exposed to Me₂SO (DMSO) or 1 nm TCDD for 8 h (A) or 50 μ M menadione for 30 min (B), labeled with DHR123, and analyzed by fluorescenceactivated cell sorter. A and B, histograms of intracellular R123 fluorescence. Histograms represent, from left to right, the autofluorescence of unstained cells (- - -), the fluorescence of DHR123-stained cells (-), and the fluorescence of cells exposed to either TCDD (A) or menadione (B) and stained with DHR123 (- with shading). C, statistical analysis of intracellular R123 fluorescence. Results are corrected for the autofluorescence of cells not labeled with DHR123 and expressed relative to the Me₂SO (DMSO) control. Bars represent the means ± S.D. of one representative experiment performed in triplicate.



enigmatic mechanisms of dioxin toxicity. Based on this expectation we performed the present study in which a 2-DE approach was used for proteome analysis. To maximize the resolving power of the gels and, thus, the sensitivity of the analysis, we made use of a set of four overlapping, narrow immobilized pH gradients for the IEF step instead of the single standard IPG strip covering a pH range of 3-10 or 4-7 commonly utilized in 2-DE studies.

In conformance with our previous ICPL study (37), we used an exposure period of 8 h to allow the detection of TCDDinduced early stimulatory effects on gene expression and, at the same time, provide sufficient time to detect a decrease in the abundance of specific proteins due to an inhibition of gene expression or an acceleration of protein degradation. This treatment scheme was also chosen to minimize possible secondary changes, such as those associated with altered cell proliferation or the induction of apoptosis, which have been reported at the transcriptome level after longer incubation periods (59).

The 2-DE approach outlined above resulted in the identification of 73 protein species with TCDD-altered abundance or PTMs. Most of the detected alterations, some of which will be discussed in the following sections, had not been described before and, as we had expected, complemented the results of the ICPL study.

Known and Putative New Members of the AhR and ARE Gene Batteries - The responsiveness of the 5L cells used in the present study to characteristic dioxin actions was clearly demonstrated by the strong induction of CYP1A1 activity and the up-regulation of several classical members of the AhR gene battery, i.e. ALDH3A1, NQO1, and, most likely, GSTA2. The genes of these enzymes contain AHRE-I in their promoter regions (60-62), and the increased expression of their cognate proteins, like that of CYP1A1, is a hallmark of the action of dioxins and other AhR agonists (63). Despite the massive enhancement of CYP1A1 activity, we detected neither

CYP1A1 nor other CYP forms known to be responsive to TCDD, such as CYP1A2 or CYP1B1 (64), among the upregulated proteins. This was not unexpected, however, because CYPs are integral proteins of the endoplasmic reticulum membrane, and their highly hydrophobic nature apparently impedes their analysis by 2-DE (65, 66). Surprisingly, however, we found CYP3A2 (which is not regarded as a member of the AhR and ARE gene batteries) among the protein spots subjected to protein identification (not shown). Its abundance was reduced by 31% and thus not considered as significantly affected by TCDD. It should yet be noted that the CYP3A2 species, which exhibited the expected molecular mass of about 60 kDa, had a pl of 5.4-5.5, which was much lower than the calculated theoretical pl of 8.9 (Scansite, Massachusetts Institute of Technology). It appears possible that the CYP3A2 spot represented a species with multiple acidic PTMs, such as phosphorylations (67, 68), which may have caused a higher hydrophilicity and its appearance on the two-dimensional gel.

Even though ALDH3A1, NQO1, and several of the TCDDinducible GST isoforms have been shown or suggested to be regulated in an AHRE-I-dependent manner, it appears unlikely that their induction in 5L cells is mediated solely via AHRE-I. The regulatory regions of the genes of rat ALDH3A1 (22), rat NQO1 (69), and the Alpha class GSTs of the rat, GSTA2 (70) and GSTA5 (71), also contain an enhancer termed ARE that is regulatable by electrophiles and oxidative stress, suggesting that ARE-dependent gene activation may also be involved in the induction of these enzymes in 5L cells. This conjecture is supported by the observed induction of GSTP1. The promoter region of rat GSTP1 does not contain AHRE-I but an enhancer designated glutathione transferase P enhancer I that is closely related to the ARE (72), and the enzyme has recently been shown to be induced via the same mechanism as ARE-dependent proteins in rat liver (73).

The expression of ARE-driven genes is mediated by the

transcription factor "nuclear factor E2 p45-related factor 2" (Nrf2) (56, 74). In a microarray study on the effect of the chemopreventive agent 3H-1,2-dithiole-3-thione, which is known to activate the Nrf2 pathway, on hepatic gene expression profiles of nrf2 wild-type and nrf2-deficient mice, Kwak et al. (47) recently identified a large number of genes regulated in an Nrf2-dependent manner. The genes included those of several well known ARE-regulated xenobiotic-metabolizing enzymes like NQO1 and GSTA2 but also a large number of others from functional classes that had not been shown previously to be inducible in an Nrf2/ARE-dependent way. Thimmulappa et al. (48) recently identified several additional genes as regulated by Nrf2 in the small intestine of mice. Among the genes identified by the two groups were several coding for proteins found to be up-regulated by TCDD in our present study, namely lamin A, tubulin β -5 chain, insulin-degrading enzyme, and transaldolase. Indirect evidence (47) suggests that the up-regulation of the β and γ subunits of the chaperonin CCT detected in the present study may also occur via the Nrf2/ARE pathway. Thus, substantially more proteins than previously thought are probably induced indirectly by TCDD in an Nrf2/ARE-dependent manner, and in view of the data of Kwak et al. (47) and Thimmulappa et al. (48) it appears highly likely that these proteins actually vastly outnumber those regulated directly by TCDD via the AHREs.

Nrf2 is normally sequestered in the cytoplasm by Keap1, a cysteine-rich protein bound to the actin cytoskeleton. Electrophiles, which alkylate specific cysteine residues of Keap1, or oxidants, which cause the formation of intersubunit disulfide bonds, dissociate Keap1 from Nrf2 resulting in nuclear translocation of Nrf2 and induction of ARE-regulated genes (56–58). The Keap1-Nrf2 complex thus acts as a sensor for electrophilic and oxidative stress. TCDD is not metabolized to electrophilic products but clearly induces the formation of reactive oxygen species in 5L cells as indicated by the intracellular oxidation of the redox-active probe DHR123. We therefore conclude that the observed increases in the abundance of proteins with ARE-containing gene promoters occurred in response to TCDD-induced oxidative stress.

It thus appears likely that the observed induction of the Nrf2/ARE-regulated proteins represents a protective mechanism against the deleterious effects of TCDD-induced ROS and their oxidizing reaction products. GSTs of the Alpha family, for example, exhibit GSH peroxidase activity (75) toward lipid hydroperoxides and use the reactive and toxic lipid peroxidation product 4-hydroxynonenal as a preferred substrate (76). The expression of GSTP1 has long been known to be regulated by the cellular redox status (77) and recently been shown to be inducible in an Nrf2-dependent manner in rat liver (73). In addition to its enzymatic function, the enzyme constitutes a sensor able to transmit redox variations to the apoptosis machinery by modulating the stress kinases pathway by inhibiting c-Jun N-terminal kinase (JNK) (78, 79). The expression of GSTP is inversely correlated with JNK activity, and

increased expression of GSTP and inhibition of JNK have been linked to the inhibition of apoptosis (78). On the other hand, oxidative stress has been shown to decrease JNK inhibition by GSTP via an oligomerization of the latter (78), to activate JNK (80), and to promote apoptosis (81). The observation that TCDD-treated 5L cells undergo apoptosis that becomes detectable after about 30 h of treatment² indicates that the observed induction of GSTP1 by TCCD is not sufficient to prevent apoptosis.

The observed up-regulation of transaldolase, another protein not previously recognized to be affected by TCDD, probably also serves to increase the antioxidant capacity of the cells in response to TCDD-induced oxidative stress. This enzyme is a key player in the regulation of the balance between the reversible non-oxidative branch of the pentose phosphate pathway and the irreversible oxidative branch. The latter is responsible for the generation of NADPH required for the maintenance of GSH in its reduced state and, thus, the protection of cells from reactive oxygen intermediates. Thimmulappa et al. (48) recently identified transaldolase as an Nrf2regulated gene in the small intestine of mice and showed that it was induced coordinately with two genes of the irreversible pathway, glucose 6-phosphate dehydrogenase and 6-phosphogluconate dehydrogenase, by the chemoprotectant sulforaphene. As both enzymes generate NADPH, the induction of transaldolase would be expected to facilitate the formation of reducing equivalents that, in turn, would maintain the antioxidative power of GSH and also directly contribute to an increased antioxidative capacity of the cells (82). Our observation that TCDD markedly stimulates glucose oxidation via the pentose phosphate pathway in 5L cells³ suggests that a mechanism similar to that described above (48) also operates in 5L cells.

Whereas the induction of ARE-regulated proteins by TCDD is generally expected to result in enhanced protection against oxidative stress, we also observed alterations of protein abundances that would be expected to enhance the susceptibility to oxidants. Thus, a protein spot identified as the aldehyde reductase, aldose reductase-related protein 2 (number 43), was down-regulated by ~50% following exposure of the cells to TCDD. The protein, also termed Akr1b8 protein or FR-1, rapidly reduces various hydrophobic aldehydes, such as 4-hydroxynonenal, as well as aromatic aldehydes (83). The expression of this enzyme, which shares some substrates with ALDH3A1 and GSTs of the Alpha family, has been shown to be positively regulated by fibroblast growth factor 1 and related peptides (84). Whether the down-regulation of aldose reductase-related protein 2 by TCDD actually reflects an interference of the dioxin with growth factor signaling remains to be determined.

Cytoskeletal Proteins - The present study corroborates our

² U. Andrae, unpublished observation

³ F. Kiefer, personal communication.

recent observation that TCDD strongly impinges on the organization of the cytoskeleton in 5L cells (37), and it markedly expands the knowledge of the proteins involved. A particularly interesting member of the group of actin-interacting proteins newly discovered to be affected by TCDD treatment was drebrin, which was down-regulated by ~50%. Drebrin has been recently identified as a connexin-43 binding partner that links gap junctions to the submembrane actin cytoskeleton and that is required for maintaining connexin-43-containing gap junctions in their functional state at the plasma membrane (85). Depletion of drebrin protein with small interfering RNA was shown to result in impaired cell-cell coupling, internalization of gap junctions, and targeting of connexin-43 for degradation (85). Thus, it appears that the down-regulation of drebrin may be conducive to the inhibition of gap junctional intercellular communication that occurs in TCDD-treated rat hepatocytes in primary culture and that has been implicated in tumor promotion by TCDD (86).

Diry et al. (87) recently reported that in human MCF7 breast cancer cells TCDD exposure resulted in morphological changes associated with a prominent cytoskeletal remodeling, increases in cell plasticity and motility, and a down-regulation of E-cadherin. Human HepG2 hepatoma cells responded similarly. These changes, which were dependent on an AhR-dependent activation of JNK and observed after a treatment period of 48 h, were tentatively linked to a potential action of dioxin on tumor progression. At present it is unclear whether the alterations of the numerous cytoskeletal proteins detected in our proteomics studies after 8 h of TCDD exposure are mechanistically related to the much later effects observed by Diry et al. (87).

Proteins Involved in the Maintenance of Mitochondrial Homeostasis - Several observations of the present and our previous studies show that TCDD exposure of 5L cells results in functionally important alterations of the mitochondrial proteome, and they suggest that some of these alterations may occur in response to the induction of mitochondrial oxidative stress. One clue is the observation of an up-regulation of the β chain of the mitochondrial ATP synthase as up-regulation of ATP synthase by toxicants has been attributed to an adaptation of the cells to mitochondrial damage induced by ROS (52, 53). For liver mitochondria of rats treated with lipopolysaccharide, up-regulation of the ATP synthase α chain was shown to be accompanied by an up-regulation of mitochondrial manganese-dependent superoxide dismutase (SOD2), and the expression of both enzymes was correlated with ROS generation suggesting that it represented a coordinated response to compensate for low levels of ATP and to increase mitochondrial antioxidant capacity (53). In fact, for rat and mouse liver, the induction of mitochondrial oxidative stress by TCDD is well established (88-91). Recent studies reported that the increased mitochondrial reactive oxygen production observed during treatment of rats with TCDD was accompanied by decreased ATP levels in the liver (90, 91). Our observations

that TCDD induces oxidative stress and up-regulates at least one of the ATP synthase subunits as well as mitochondrial superoxide dismutase (37) in 5L cells suggest that a similar ROS-dependent adaptive mechanism is operative in mitochondria of TCDD-exposed 5L cells.

The notion that TCDD causes an imbalance in ATP demand and supply in 5L cells is indirectly supported by results from our previous ICPL study (37), which had revealed an interference by TCDD with the abundance or PTM of ADP/ATP translocase 1 (ANT1), a component of the inner mitochondrial membrane, and the glycolytic enzyme hexokinase I. ANT1 and the mitochondrial hexokinases I and II (HKI and HKII) interact with the VDACs of the outer mitochondrial membrane (92-94) that constitute the major pores for metabolic exchange of ATP, ADP, and inorganic phosphate and that have been suggested to act as dynamic regulators of global mitochondrial function by ultimately controlling the activity of the respiratory chain (95). The observed TCDD-induced alterations of ANT1 and HKI may thus indicate an interference of TCDD with the function of VDAC, although the precise nature of the alterations remains to be defined.

A particularly important outcome of the present study was the discovery that TCDD markedly affects the VDAC isoform VDAC2 in 5L cells. VDAC2, in addition to its function as a pore, mediates the import of the proapoptotic protein BAK into the outer mitochondrial membrane (54), inhibits the activity of BAK by preventing its oligomerization (55), and, thus, provides a connection between mitochondrial physiology and the core apoptotic pathway. Our data show that TCDD exposure results in both an altered PTM of VDAC2 and a marked increase in its abundance. The nature of the difference of the two forms of VDAC2, which may be related to the two VDAC2 species detected by 2-DE analysis of various rat tissues by Yamamoto et al. (96), is still unclear. VDAC2 is known to be subject to tyrosine phosphorylation (97) and lysine acetylation (98), but the very small pl difference of the two observed spots of <0.1 pH unit suggests that the two forms do not differ by one of these PTMs but, presumably, some other modification.

Up-regulation of VDAC2 protein was dependent on the AhR in 5L cells as indicated by the absence of any effect of TCDD on the amount of VDAC2 in the AhR-deficient 5L subline BP8. In contrast to the proteins of the AhR and ARE gene batteries that are regulated at the level of transcription, quantitative PCR analyses showed that up-regulation of VDAC2 was not mediated by an increase in the steady-state level of VDAC2 mRNA. We therefore suppose that the increase in the amount of VDAC2 protein during exposure to TCDD occurs at the translational level or via a prolongation of the half-life of the protein. We are not aware of any other report on an increase in VDAC2 protein in cells in response to exposure to chemicals such as drugs or xenobiotics. VDAC2 was one of a large number of genes of mouse cerebral cortical neurons with increased expression in response to hypoxia (99), but as this increase occurred at the transcriptional level it must have been mediated by a different mechanism. Because retroviral overexpression of VDAC2 has been shown to result in an inhibition of the mitochondrial apoptotic pathway via an inhibition of BAK activation (55), the up-regulation of VDAC2 protein observed in our study may constitute a general, hitherto unrecognized component of a concerted endeavor of cells to prevent cell death due to an imbalance between cellular energy demand and mitochondrial ATP supply. As the function of VDAC2 as a pore in the outer mitochondrial membrane is shared with that of the more abundant (96) VDAC1, the increased capability of the cells to keep BAK in check may be more momentous than the increase in permeability for metabolic exchange provided by the up-regulation of VDAC2 protein.

Taken together, our findings indicate that within 8 h of treatment TCDD induces concerted changes in the mitochondrial proteome that probably occur to counteract oxidative stress, to prevent ROS-induced energy depletion, and to maintain cell viability by sustaining ATP supply and inhibiting the triggering of the intrinsic, mitochondria-mediated apoptotic pathway. The observation that the cells nevertheless undergo apoptosis that becomes detectable in TCCD-exposed 5L cells after about 30 h of treatment² shows, however, that these alterations cannot prevent TCDD-induced cell death in the long run.

Comparison of the Results with Those from the ICPL Study (37)-In our previous ICPL study on the effects of TCDD on the proteome of 5L cells that used cell culture and treatment conditions identical to those of the present investigation, 89 different proteins were identified as up- or down-regulated by TCDD (37). This figure is similar to the number of 78 protein species, which corresponded to 73 different proteins, detected as "regulated" in the present study. Interestingly an inspection of the two protein lists reveals that the overlap between the two studies, i.e. the number of proteins detected by both methods, amounted to only nine (numbers 6, 9, 35, 42, 50, and 57-60). Of the 80 proteins detected only by the ICPL method, 27 proteins, largely histones and ribosomal proteins, had pl values above 9.5 and would thus be expected to cause problems in 2-DE analyses. Five had a molecular mass of >200 kDa and seven had a molecular mass of <15 kDa and were, therefore, also outside the range readily amenable to standard 2-DE analysis. Of the remaining 41 proteins, several may have been too hydrophobic for an analysis by 2-DE, but for the majority of them there is no straightforward explanation why they were not detected in the present study. Conversely it is not readily apparent why 64 altered proteins were only detected using the 2-DE but not the ICPL method. However, this limited concordance is actually not too surprising as several studies have shown that the choice of the methodology used for global proteome analysis strongly affects the spectrum of proteins detected (compare e.g. Refs. 38, 39, and 100). The results of our investigations on the impact of TCDD on the proteome of 5L cells demonstrate that

the concurrent use of the ICPL and the 2-DE approach for quantitative proteome analysis can in fact yield highly complementary information on a biological system under study.

* The costs of publication of this article were defrayed in part by the payment of page charges. This article must therefore be hereby marked "advertisement" in accordance with 18 U.S.C. Section 1734 solely to indicate this fact.

S The on-line version of this article (available at http://www.mcponline.org) contains supplemental material.

¶ To whom correspondence should be addressed: GSF-Forschungszentrum für Umwelt und Gesundheit, Institut für Toxikologie, Ingolstädter Landstr. 1, D-85764 Neuherberg, Germany. Tel.: 49-89-3187-2221; Fax: 49-89-3187-3449; E-mail: andrae@gsf.de.

REFERENCES

- Gold, L. S., Slone, T. H., Manley, N. B., Garfinkel, G. B., Hudes, E. S., Rohrbach, L., and Ames, B. N. (1991) The Carcinogenic Potency Database, analyses of 4000 chronic animal cancer experiments published in the general literature and by the U.S. National Cancer Institute/National Toxicology Program. *Environ. Health Perspect.* 96, 11–15
- International Agency for Research on Cancer (IARC) (1997) IARC Monographs on the Evaluation of Carcinogenic Risks to Humans: Polychlorinated Dibenzo-para-dioxins and Polychlorinated Dibenzofurans, Vol. 69, International Agency for Research on Cancer, Lyon, France
- Steenland, K., Bertazzi, P., Baccarelli, A., and Kogevinas, M. (2004) Dioxin revisited: developments since the 1997 IARC classification of dioxin as a human carcinogen. *Environ. Health Perspect.* 112, 1265–1268
- Whitlock, J. P., Jr. (1999) Induction of cytochrome P4501A1. Annu. Rev. Pharmacol. Toxicol. 39, 103–125
- Safe, S. (2001) Molecular biology of the Ah receptor and its role in carcinogenesis. *Toxicol. Lett.* 120, 1–7
- Sogawa, K., Numayama-Tsuruta, K., Takahashi, T., Matsushita, N., Miura, C., Nikawa, J., Gotoh, O., Kikuchi, Y., and Fujii-Kuriyama, Y. (2004) A novel induction mechanism of the rat CYP1A2 gene mediated by Ah receptor-Arnt heterodimer. *Biochem. Biophys. Res. Commun.* 318, 746–755
- Boutros, P. C., Moffat, I. D., Franc, M. A., Tijet, N., Tuomisto, J., Pohjan-virta, R., and Okey, A. B. (2004) Dioxin-responsive AHRE-II gene battery, identification by phylogenetic footprinting. *Biochem. Biophys. Res. Commun.* 321, 707–715
- Radjendirane, V., and Jaiswal, A. K. (1999) Antioxidant response element-mediated 2,3,7,8-tetrachlorodibenzo-p-dioxin (TCDD) induction of human NAD(P)H:quinone oxidoreductase 1 gene expression. *Biochem. Pharmacol.* 58, 1649–1655
- Enan, E., and Matsumura, F. (1996) Identification of c-Src as the integral component of the cytosolic Ah receptor complex, transducing the signal of 2,3,7,8-tetrachlorodibenzo-p-dioxin (TCDD) through the protein phosphorylation pathway. *Biochem. Pharmacol.* 52, 1599–1612
- Puga, A., Barnes, S. J., Dalton, T. P., Chang, C., Knudsen, E. S., and Maier, M. A. (2000) Aromatic hydrocarbon receptor interaction with the retinoblastoma protein potentiates repression of E2F-dependent transcription and cell cycle arrest. J. Biol. Chem. 275, 2943–2950
- Weiss, C., Faust, D., Durk, H., Kolluri, S. K., Pelzer, A., Schneider, S., Dietrich, C., Oesch, F., and Göttlicher, M. (2005) TCDD induces c-jun expression via a novel Ah (dioxin) receptor-mediated p38-MAPK-dependent pathway. *Oncogene* 24, 4975–4983
- Puga, A., Maier, A., and Medvedovic, M. (2000) The transcriptional signature of dioxin in human hepatoma HepG2 cells. *Biochem. Pharmacol.* 60, 1129–1142
- Frueh, F. W., Hayashibara, K. C., Brown, P. O., and Whitlock, J. P., Jr. (2001) Use of cDNA microarrays to analyze dioxin-induced changes in human liver gene expression. *Toxicol. Lett.* 122, 189–203
- Kolluri, S. K., Balduf, C., Hofmann, M., and Göttlicher, M. (2001) Novel target genes of the Ah (dioxin) receptor, transcriptional induction of N-myristoyltransferase 2. Cancer Res. 61, 8534–8539
- Kurachi, M., Hashimoto, S., Obata, A., Nagai, S., Nagahata, T., Inadera, H., Sone, H., Tohyama, C., Kaneko, S., Kobayashi, K., and Matsushima, K. (2002) Identification of 2,3,7,8-tetrachlorodibenzo-p-dioxin-respon-

- sive genes in mouse liver by serial analysis of gene expression. *Biochem. Biophys. Res. Commun.* **292,** 368–377
- Zeytun, A., McKallip, R. J., Fisher, M., Camacho, I., Nagarkatti, M., and Nagarkatti, P. S. (2002) Analysis of 2,3,7,8-tetrachlorodibenzo-p-dioxininduced gene expression profile in vivo using pathway-specific cDNA arrays. *Toxicology* 178, 241–260
- Boverhof, D. R., Burgoon, L. D., Tashiro, C., Chittim, B., Harkema, J. R., Jump, D. B., and Zacharewski, T. R. (2005) Temporal and dose-dependent hepatic gene expression patterns in mice provide new insights into TCDD-mediated hepatotoxicity. *Toxicol. Sci.* 85, 1048–1063
- Boverhof, D. R., Burgoon, L. D., Tashiro, C., Sharratt, B., Chittim, B., Harkema, J. R., Mendrick, D. L., and Zacharewski, T. R. (2006) Comparative toxicogenomic analysis of the hepatotoxic effects of TCDD in Sprague Dawley rats and C57BL/6 mice. *Toxicol. Sci.* 94, 398–416
- Fletcher, N., Wahlstrom, D., Lundberg, R., Nilsson, C. B., Nilsson, K. C., Stockling, K., Hellmold, H., and Hakansson, H. (2005) 2,3,7,8-Tetrachlorodibenzo-p-dioxin (TCDD) alters the mRNA expression of critical genes associated with cholesterol metabolism, bile acid biosynthesis, and bile transport in rat liver, a microarray study. *Toxicol. Appl. Pharmacol.* 207, 1–24
- Tijet, N., Boutros, P. C., Moffat, I. D., Okey, A. B., Tuomisto, J., and Pohjanvirta, R. (2006) Aryl hydrocarbon receptor regulates distinct dioxindependent and dioxin-independent gene batteries. *Mol. Pharmacol.* 69, 140–153
- Lee, S. H., Lee, D. Y., Son, W. K., Joo, W. A., and Kim, C. W. (2005) Proteomic characterization of rat liver exposed to 2,3,7,8-tetrachlorobenzo-p-dioxin. J. Proteome Res. 4, 335–343
- Pastorelli, R., Carpi, D., Campagna, R., Airoldi, L., Pohjanvirta, R., Viluksela, M., Hakansson, H., Boutros, P. C., Moffat, I. D., Okey, A. B., and Fanelli, R. (2006) Differential expression profiling of the hepatic proteome in a rat model of dioxin resistance, correlation with genomic and transcriptomic analyses. *Mol. Cell. Proteomics* 5, 882–894
- Oberemm, A., Meckert, C., Brandenburger, L., Herzig, A., Lindner, Y., Kalenberg, K., Krause, E., Ittrich, C., Kopp-Schneider, A., Stahlmann, R., Richter-Reichhelm, H. B., and Gundert-Remy, U. (2005) Differential signatures of protein expression in marmoset liver and thymus induced by single-dose TCDD treatment. *Toxicology* 206, 33–48
- Wildgruber, R., Harder, A., Obermaier, C., Boguth, G., Weiss, W., Fey, S. J., Larsen, P. M., and Görg, A. (2000) Towards higher resolution, two-dimensional electrophoresis of Saccharomyces cerevisiae proteins using overlapping narrow immobilized pH gradients. *Electrophoresis* 21, 2610–2616
- Görg, A., Weiss, W., and Dunn, M. J. (2004) Current two-dimensional electrophoresis technology for proteomics. *Proteomics* 4, 3665–3685
- Göttlicher, M., Cikryt, P., and Wiebel, F. J. (1990) Inhibition of growth by 2,3,7,8-tetrachlorodibenzo-p-dioxin in 5L rat hepatoma cells is associated with the presence of Ah receptor. Carcinogenesis 11, 2205–2210
- Göttlicher, M., and Wiebel, F. J. (1991) 2,3,7,8-Tetrachlorodibenzo-pdioxin causes unbalanced growth in 5L rat hepatoma cells. *Toxicol. Appl. Pharmacol.* 111, 496-503
- Wiebel, F. J., Klose, U., and Kiefer, F. (1991) Toxicity of 2,3,7,8-tetrachlorodibenzo-p-dioxin in vitro, H4IIEC3-derived 5L hepatoma cells as a model system. *Toxicol. Lett.* 55, 161–169
- Weiss, C., Kolluri, S. K., Kiefer, F., and Göttlicher, M. (1996) Complementation of Ah receptor deficiency in hepatoma cells, negative feedback regulation and cell cycle control by the Ah receptor. *Exp. Cell Res.* 226, 154–163
- Ge, N. L., and Elferink, C. J. (1998) A direct interaction between the aryl hydrocarbon receptor and retinoblastoma protein. *J. Biol. Chem.* 273, 22708–22713
- Reiners, J. J., Jr., Clift, R., and Mathieu, P. (1999) Suppression of cell cycle progression by flavonoids: dependence on the aryl hydrocarbon receptor. *Carcinogenesis* 20, 1561–1566
- Elferink, C. J., Ge, N. L., and Levine, A. (2001) Maximal aryl hydrocarbon receptor activity depends on an interaction with the retinoblastoma protein. Mol. Pharmacol. 59, 664–673
- Levine-Fridman, A., Chen, L., and Elferink, C. J. (2004) Cytochrome P4501A1 promotes G1 phase cell cycle progression by controlling aryl hydrocarbon receptor activity. Mol. Pharmacol. 65, 461–469
- Munzel, P. A., Schmohl, S., Buckler, F., Jaehrling, J., Raschko, F. T., Köhle, C., and Bock, K. W. (2003) Contribution of the Ah receptor to the

- phenolic antioxidant-mediated expression of human and rat UDP-glucuronosyltransferase UGT1A6 in Caco-2 and rat hepatoma 5L cells. *Biochem. Pharmacol.* **66,** 841–847
- Kolluri, S. K., Weiss, C., Koff, A., and Göttlicher, M. (1999) p27 (Kip1) induction and inhibition of proliferation by the intracellular Ah receptor in developing thymus and hepatoma cells. Genes Dev. 13, 1742–17453
- Schmidt, A., Kellermann, J., and Lottspeich, F. (2005) A novel strategy for quantitative proteomics using isotope-coded protein labels. *Proteomics* 5, 4–15
- Sarioglu, H., Brandner, S., Jacobsen, C., Meindl, T., Schmidt, A., Kellermann, J., Lottspeich, F., and Andrae, U. (2006) Quantitative analysis of 2,3,7,8-tetrachlorodibenzo-p-dioxin-induced proteome alterations in 5L rat hepatoma cells using isotope-coded protein labels. *Proteomics* 6, 2407–2421
- DeSouza, L., Diehl, G., Rodrigues, M. J., Guo, J., Romaschin, A. D., Colgan, T. J., and Siu, K. W. (2005) Search for cancer markers from endometrial tissues using differentially labeled tags iTRAQ and clCAT with multidimensional liquid chromatography and tandem mass spectrometry. J. Proteome Res. 4, 377–386
- Wu, W., Wang, G., Baek, S. J., and Shen, R. F. (2006) Comparative study of three proteomic quantitative methods, DIGE, cICAT, and iTRAQ, using 2D gel- or LC-MALDI TOF/TOF. J. Proteome Res. 5, 651–658
- Moore, E. E., and Weiss, M. C. (1982) Selective isolation of stable and unstable dedifferentiated variants from a rat hepatoma cell line. *J. Cell. Physiol.* 111, 1–8
- Pitot, H., Peraino, C., Morse, P. A., and Potter, V. E. (1964) Hepatomas in tissue culture compared with adapting liver in vivo. *Natl. Cancer Inst. Monogr.* 13, 229–246
- Reuber, M. D., (1961) A transplantable bile-secreting hepatocellular carcinoma in the rat. J. Natl. Cancer Inst. 26, 891–900
- Lamanda, A., Zahn, A., Roder, D., and Langen, H. (2004) Improved ruthenium II tris (bathophenantroline disulfonate) staining and destaining protocol for a better signal-to-background ratio and improved baseline resolution. *Proteomics* 4, 599–608
- Shevchenko, A., Wilm, W., Vorm, O., and Mann, M. (1996) Mass spectrometric sequencing of proteins from silver-stained polyacrylamide gels. *Anal. Chem.* 68, 850–858
- Hauck, S. M., Ekstrom, P. A., Ahuja-Jensen, P., Suppmann, S., Paquet-Durand, F., van Veen, T., and Ueffing, M. (2006) Differential modification of phosducin protein in degenerating rd1 retina is associated with constitutively active Ca²⁺/calmodulin kinase II in rod outer segments. *Mol. Cell. Proteomics* 5, 324–336
- Miao, W., Hu, L., Kandouz, M., and Batist, G. (2003) Oltipraz is a bifunctional inducer activating both phase I and phase II drug-metabolizing enzymes via the xenobiotic responsive element. *Mol. Pharmacol.* 64, 346–354
- Kwak, M. K., Wakabayashi, N., Itoh, K, Motohashi, H., Yamamoto, M., and Kensler, T. W. (2003) Modulation of gene expression by cancer chemopreventive dithiolethiones through the Keap1-Nrf2 pathway. Identification of novel gene clusters for cell survival. *J. Biol. Chem.* 278, 8135–8145
- Thimmulappa, R. K., Mai, K. H., Srisuma, S., Kensler, T. W., Yamamoto, M., and Biswal, S. (2002) Identification of Nrf2-regulated genes induced by the chemopreventive agent sulforaphane by oligonucleotide microarray. *Cancer Res.* 62, 5196–5203
- 49. Ellis, E. M., Slattery, C. M., and Hayes, J. D. (2003) Characterization of the rat aflatoxin B1 aldehyde reductase gene, AKR7A1. Structure and chromosomal localization of AKR7A1 as well as identification of antioxidant response elements in the gene promoter. Carcinogenesis 24, 727–737
- Dos Remedios, C. G., Chhabra, D., Kekic, M., Dedova, I. V., Tsubakihara, M., Berry, D. A., and Nosworthy, N. J. (2003) Actin binding proteins: regulation of cytoskeletal microfilaments. *Physiol. Rev.* 83, 433–473
- Valpuesta, J. M., Martin-Benito, J., Gomez-Puertas, P., Carrascosa, J. L., and Willison, K. R. (2002) Structure and function of a protein folding machine, the eukaryotic cytosolic chaperonin CCT. FEBS Lett. 529, 11–16.
- 52. Yu, J. H., Yun, S. Y., Lim, J. W., Kim, H., and Kim, K. H. (2003) Mass spectrometry and tandem mass spectrometry analysis of rat mitochondrial ATP synthase, up-regulation in pancreatic acinar cells treated with cerulein. *Proteomics* **3**, 2437–2445
- 53. Miller, I., Gemeiner, M., Gesslbauer, B., Kungl, A., Piskernik, C., Haindl, S.,

- Nurnberger, S., Bahrami, S., Redl, H., and Kozlov, A. V. (2006) Proteome analysis of rat liver mitochondria reveals a possible compensatory response to endotoxic shock. *FEBS Lett.* **580**, 1257–1262
- Setoguchi, K., Otera, H., and Mihara, K. (2006) Cytosolic factor- and TOM-independent import of C-tail-anchored mitochondrial outer membrane proteins. EMBO J. 25, 5635–5647
- Cheng, E. H., Sheiko, T. V., Fisher, J. K., Craigen, W. J., and Korsmeyer, S. J. (2003) VDAC2 inhibits BAK activation and mitochondrial apoptosis. Science 301, 513–517
- Ishii, T., Itoh, K., Takahashi, S., Sato, H., Yanagawa, T., Katoh, Y., Bannai, S., and Yamamoto, M. (2000) Transcription factor Nrf2 coordinately regulates a group of oxidative stress-inducible genes in macrophages. J. Biol. Chem. 275, 16023–16029
- 57. Wakabayashi, N., Dinkova-Kostova, A. T., Holtzclaw, W. D., Kang, M. I., Kobayashi, A., Yamamoto, M., Kensler, T. W., and Talalay, P. (2004) Protection against electrophile and oxidant stress by induction of the phase 2 response: fate of cysteines of the Keap1 sensor modified by inducers. *Proc. Natl. Acad. Sci. U. S. A.* 101, 2040–2045
- Kang, K. W., Lee, S. J., and Kim, S. G. (2005) Molecular mechanism of nrf2 activation by oxidative stress. *Antioxid. Redox Signal.* 7, 1664–1673
- Hanlon, P. R., Zheng, W., Ko, A. Y., and Jefcoate, C. R. (2005) Identification of novel TCDD-regulated genes by microarray analysis. *Toxicol. Appl. Pharmacol.* 202, 215–228
- Boesch, J. S., Miskimins, R., Miskimins, W. K., and Lindahl, R. (1999) The same xenobiotic response element is required for constitutive and inducible expression of the mammalian aldehyde dehydrogenase-3 gene. Arch. Biochem. Biophys. 361, 223–230
- Favreau, L. V., and Pickett, C. B. (1991) Transcriptional regulation of the rat NAD(P)H:quinone reductase gene. Identification of regulatory elements controlling basal level expression and inducible expression by planar aromatic compounds and phenolic antioxidants. J. Biol. Chem. 266, 4556–4561
- Rushmore, T. H., King, R. G., Paulson, K. E., and Pickett, C. B. (1990) Regulation of glutathione S-transferase Ya subunit gene expression, identification of a unique xenobiotic-responsive element controlling inducible expression by planar aromatic compounds. *Proc. Natl. Acad.* Sci. U. S. A. 87, 3826–3830
- Schrenk, D. (1998) Impact of dioxin-type induction of drug-metabolizing enzymes on the metabolism of endo- and xenobiotics. *Biochem. Phar-macol.* 55, 1155–1162
- Santostefano, M. J., Ross, D. G., Savas, U., Jefcoate, C. R., and Birn-baum, L. S. (1997) Differential time-course and dose-response relationships of TCDD-induced CYP1B1, CYP1A1, and CYP1A2 proteins in rats. *Biochem. Biophys. Res. Commun.* 233, 20–24
- Fountoulakis, M., Juranville, J. F., Berndt, P., Langen, H., and Suter, L. (2001) Two-dimensional database of mouse liver proteins. An update. *Electrophoresis* 22, 1747–1763
- Fountoulakis, M., and Suter, L. (2002) Proteomic analysis of the rat liver.
 J. Chromatogr. B Anal. Technol. Biomed. Life Sci. 782, 197–218
- Eliasson, E., Mkrtchian, S., Halper, J. R., and Ingelman-Sundberg, M. (1994) Substrate-regulated, cAMP-dependent phosphorylation, denaturation, and degradation of glucocorticoid-inducible rat liver cytochrome P450 3A1. J. Biol. Chem. 269, 18378–18383
- Wang, X., Medzihradszky, K. F., Maltby, D., and Correia, M. A. (2001) Phosphorylation of native and heme-modified CYP3A4 by protein kinase C, a mass spectrometric characterization of the phosphorylated peptides. *Biochemistry* 40, 11318–11326
- Favreau, L. V., and Pickett, C. B. (1993) Transcriptional regulation of the rat NAD(P)H:quinone reductase gene. Characterization of a DNA-protein interaction at the antioxidant responsive element and induction by 12-O-tetradecanoylphorbol 13-acetate. J. Biol. Chem. 268, 19875–19881
- Rushmore, T. H., Morton, M. R., and Pickett, C. B. (1991) The antioxidant responsive element. Activation by oxidative stress and identification of the DNA consensus sequence required for functional activity. *J. Biol. Chem.* 266, 11632–11639
- Pulford, D. J., and Hayes, J. D. (1996) Characterization of the rat glutathione S-transferase Yc2 subunit gene, GSTA5, identification of a putative antioxidant-responsive element in the 5'-flanking region of rat GSTA5 that may mediate chemoprotection against aflatoxin B1. *Bio*chem. J. 318, 75–84

- Okuda, A., Imagawa, M., Maeda, Y., Sakai, M., and Muramatsu, M. (1989) Structural and functional analysis of an enhancer GPEI having a phorbol 12-O-tetradecanoate 13-acetate responsive element-like sequence found in the rat glutathione transferase P gene. J. Biol. Chem. 264, 16919–16926
- Yates, M. S., Kwak, M. K., Egner, P. A., Groopman, J. D., Bodreddigari, S., Sutter, T. R., Baumgartner, K. J., Roebuck, B. D., Liby, K. T., Yore, M. M., Honda, T., Gribble, G. W., Sporn, M. B., and Kensler, T. W. (2006) Potent protection against aflatoxin-induced tumorigenesis through induction of Nrf2-regulated pathways by the triterpenoid 1-[2-cyano-3-, 12-dioxooleana-1,9(11)-dien-28-oyl]imidazole. Cancer Res. 66, 2488-2494
- Itoh, K., Chiba, T., Takahashi, S., Ishii, T., Igarashi, K., Katoh, Y., Oyake, T., Hayashi, N., Satoh, K., Hatayama, I., Yamamoto, M., and Nabeshima, Y. (1997) An Nrf2/small Maf heterodimer mediates the induction of phase II detoxifying enzyme genes through antioxidant response elements. Biochem. Biophys. Res. Commun. 236, 313–322
- Arthur, J. R., Morrice, P. C., Nicol, F., Beddows, S. E., Boyd, R., Hayes, J. D., and Beckett, G. J. (1987) The effects of selenium and copper deficiencies on glutathione S-transferase and glutathione peroxidase in rat liver. *Biochem. J.* 248, 539–544
- Khan, M. F., Srivastava, S. K., Singhal, S. S., Chaubey, M., Awasthi, S., Petersen, D. R., Ansari, G. A., and Awasthi, Y. C. (1995) Iron-induced lipid peroxidation in rat liver is accompanied by preferential induction of glutathione S-transferase 8–8 isozyme. *Toxicol. Appl. Pharmacol.* 131, 63–72
- Xia, C., Hu, J., Ketterer, B., and Taylor, J. B. (1996) The organization of the human GSTP1–1 gene promoter and its response to retinoic acid and cellular redox status. *Biochem. J.* 313, 155–161
- Adler, V., Yin, Z., Fuchs, S. Y., Benezra, M., Rosario, L., Tew, K. D., Pincus, M. R., Sardana, M., Henderson, C. J., Wolf, C. R., Davis, R. J., and Ronai, Z. (1999) Regulation of JNK signaling by GSTp. *EMBO J.* 18, 132113–132134
- Wang, T., Arifoglu, P., Ronai, Z., and Tew, K. D. (2001) Glutathione S-transferase P1–1 (GSTP1–1) inhibits c-Jun N-terminal kinase (JNK1) signaling through interaction with the C terminus. *J. Biol. Chem.* 276, 20999–21003
- Devary, Y., Gottlieb, R. A., Smeal, T., and Karin, M. (1992) The mammalian ultraviolet response is triggered by activation of Src tyrosine kinases. *Cell* 71, 1081–1091
- Xia, Z., Dickens, M., Raingeaud, J., Davis, R. J., and Greenberg, M. E. (1995) Opposing effects of ERK and JNK-p38 MAP kinases on apoptosis. Science 270, 1326–1331
- Kirsch, M., and De Groot, H. (2001) NAD(P)H, a directly operating antioxidant? FASEB J. 15, 1569–1574
- Srivastava, S., Harter, T. M., Chandra, A., Bhatnagar, A., Srivastava, S. K., and Petrash, J. M. (1998) Kinetic studies of FR-1, a growth factorinducible aldo-keto reductase. *Biochemistry* 37, 12909–12917
- Donohue, P. J., Alberts, G. F., Hampton, B. S., and Winkles, J. A. (1994)
 A delayed-early gene activated by fibroblast growth factor-1 encodes a protein related to aldose reductase. J. Biol. Chem. 269, 8604–8609
- Butkevich, E., Hülsmann, S., Wenzel, D., Shirao, T., Duden, R., and Majoul, I. (2004) Drebrin is a novel connexin-43 binding partner that links gap junctions to the submembrane cytoskeleton. *Curr. Biol.* 14, 650–658
- Baker, T. K., Kwiatkowski, A. P., Madhukar, B. V., and Klaunig, J. E. (1995) Inhibition of gap junctional intercellular communication by 2,3,7,8-tetrachlorodibenzo-p-dioxin (TCDD) in rat hepatocytes. *Carcinogenesis* 16, 2321–2326
- 87. Diry, M., Tomkiewicz, C., Koehle, C., Coumoul, X., Bock, K. W., Barouki, R., and Transy, C. (2006) Activation of the dioxin/aryl hydrocarbon receptor (AhR) modulates cell plasticity through a JNK-dependent mechanism. *Oncogene* **25**, 5570–5574
- Stohs, S. J., Alsharif, N. Z., Shara, M. A., al-Bayati, Z. A., and Wahba, Z. Z. (1991) Evidence for the induction of an oxidative stress in rat hepatic mitochondria by 2,3,7,8-tetrachlorodibenzo-p-dioxin (TCDD). Adv. Exp. Med. Biol. 283, 827–831
- Senft, A. P., Dalton, T. P., Nebert, D. W., Genter, M. B., Hutchinson, R. J., and Shertzer, H. G. (2002) Dioxin increases reactive oxygen production in mouse liver mitochondria. *Toxicol. Appl. Pharmacol.* 178, 15–21
- 90. Shen, D., Dalton, T. P., Nebert, D. W., and Shertzer, H. G. (2005) Gluta-

- thione redox state regulates mitochondrial reactive oxygen production. J. Biol. Chem. 280, 25305–25312
- Shertzer, H. G., Genter, M. B., Shen, D., Nebert, D. W., Chen, Y., and Dalton, T. P. (2006) TCDD decreases ATP levels and increases reactive oxygen production through changes in mitochondrial F₀F₁-ATP synthase and ubiquinone. *Toxicol. Appl. Pharmacol.* 217, 363–374
- 92. Baines, C. P., Song, C. X., Zheng, Y. T., Wang, G. W., Zhang, J., Wang, O. L., Guo, Y., Bolli, R., Cardwell, E. M., and Ping, P. (2003) Protein kinase $C_{\mathcal{E}}$ interacts with and inhibits the permeability transition pore in cardiac mitochondria. *Circ. Res.* **92**, 873–880
- Majewski, N., Nogueira, V., Bhaskar, P., Coy, P. E., Skeen, J. E., Gottlob, K., Chandel, N. S., Thompson, C. B., Robey, R. B., and Hay, N. (2004) Hexokinase-mitochondria interaction mediated by Akt is required to inhibit apoptosis in the presence or absence of Bax and Bak. *Mol. Cell* 16, 819–830
- Robey, R. B., and Hay, N. (2006) Mitochondrial hexokinases, novel mediators of the antiapoptotic effects of growth factors and Akt. *Oncogene* 25, 4683–4696
- Lemasters, J. J., and Holmuhamedov, E. (2006) Voltage-dependent anion channel (VDAC) as mitochondrial governator—thinking outside the box. *Biochim. Biophys. Acta* 1762, 181–190
- 96. Yamamoto, T., Yamada, A., Watanabe, M., Yoshimura, Y., Yamazaki, N.,

- Yoshimura, Y., Yamauchi, T., Kataoka, M., Nagata, T., Terada, H., and Shinohara, Y. (2006) VDAC1, having a shorter N-terminus than VDAC2 but showing the same migration in an SDS-polyacrylamide gel, is the predominant form expressed in mitochondria of various tissues. *J. Proteome Res.* **5**, 3336–3344
- 97. Liberatori, S., Canas, B., Tani, C., Bini, L., Buonocore, G., Godovac-Zimmermann, J., Mishra, O. P., Delivoria-Papadopoulos, M., Bracci, R., and Pallini, V. (2004) Proteomic approach to the identification of voltage-dependent anion channel protein isoforms in guinea pig brain synaptosomes. *Proteomics* 4, 1335–1340
- Kim, S. C., Sprung, R., Chen, Y., Xu, Y., Ball, H., Pei, J., Cheng, T., Kho, Y., Xiao, H., Xiao, L., Grishin, N. V., White, M., Yang, X. J., and Zhao, Y. (2006) Substrate and functional diversity of lysine acetylation revealed by a proteomics survey. *Mol. Cell* 23, 607–618
- Jin, K., Mao, X. O., Eshoo, M. W., del Rio, G., Rao, R., Chen, D., Simon, R. P., and Greenberg, D. A. (2002) cDNA microarray analysis of changes in gene expression induced by neuronal hypoxia in vitro. *Neurochem. Res.* 27, 1105–1112
- Wolff, S., Otto, A., Albrecht, D., Zeng, J. S., Buttner, K., Gluckmann, M., Hecker, M., and Becher, D. (2006) Gel-free and gel-based proteomics in Bacillus subtilis, a comparative study. *Mol. Cell. Proteomics.* 5, 1183–1192